
ZEROTH-ORDER ADAPTIVE NEURON ALIGNMENT BASED PRUNING WITHOUT RE-TRAINING

Elia Cunegatti, Leonardo Lucio Custode, Giovanni Iacca,
 Department of Information Engineering and Computer Science
 University of Trento, Italy
 {elia.cunegatti, leonardo.custode, giovanni.iacca}@unitn.it

ABSTRACT

Network pruning is a set of computational techniques that aim to reduce a given model’s computational cost by removing a subset of its parameters while having minimal impact on performance. Throughout the last decade, the most widely used pruning paradigm has focused on pruning and re-training, which nowadays is inconvenient due to the vast amount of pre-trained models, which are in any case too expensive to re-train. In this paper, we exploit functional information from dense pre-trained models, i.e., their activations, to obtain sparse models that maximize the activations’ alignment w.r.t. their corresponding dense models. Hence, we propose NEURONAL, a *top-up* algorithm that can be used on top of any given pruning algorithm for LLMs, that modifies the block-wise and row-wise sparsity ratios to maximize the *neuron alignment* among activations. Moreover, differently from existing methods, our approach adaptively selects the best parameters for the block-wise and row-wise sparsity ratios w.r.t. to the model and the desired sparsity (given as input), and requires *no re-training*. We test our method on 4 different LLM families and 3 different sparsity ratios, showing how it consistently outperforms the latest state-of-the-art techniques. The code is available at <https://github.com/eliacunegatti/NeuroAL>.

1 Introduction

In recent times, Large Language Models (LLMs) have shown incredible performance over almost any language task [44, 33, 4]. However, their performance tends to grow with their sizes (i.e., the number of trainable parameters), which in turn is proportional to the computational burden required to train and then use such models. One way to reduce the computational cost of LLMs is through *network pruning*, i.e., algorithms that remove parameters while minimizing performance degradation. This approach has been extensively studied on Convolutional Neural Networks (CNNs) [13, 25, 43, 11], but nowadays the focus has shifted towards pre-trained models [41, 42, 22]. This shift has required a change of paradigm in pruning techniques: in fact, while in CNNs the main paradigm is iterative pruning (with re-training) [13], with pre-trained models (such as LLMs) in most cases it is not possible to fully re-train such models, because (1) training data are often not accessible, and (2) full re-training would be anyway too expensive. This calls for “exploiting” as much as possible the information contained in a pre-trained model to obtain a performant sparse version of it, using weight’s information [21], activations [40, 39], or reconstruction error [15], without the need for re-training. More recently, a new category of pruning algorithms, which we may call *top-up* algorithms (i.e., methods that can be applied on top of a given pruning algorithm for LLMs), has emerged, aiming at further improving pruning performance. Such approaches can be divided into two categories: those that minimize the reconstruction error [18, 45, 49], and those that impose non-uniform sparsity distribution modifying the block-wise sparsity [46]. The latter category is extremely effective for improving performance in CNNs [14, 38], while its application to LLMs is still limited [46].

Contributions In this paper, we first analyze the reasons behind the effectiveness of non-uniform sparsity distribution in sparse LLM. To do so, we carefully analyze the state-of-the-art top-up method OWL [46], investigating the reason underlying its better performance (w.r.t. other methods from the state of the art) as well as its limitations in terms of sensitiveness to its hyperparameters. Leveraging this knowledge, we introduce a new top-up method, that we call NEURONAL. The algorithm consists of a two-step approach that re-distributes the block-wise sparsity, i.e., the sparsity among Transformer blocks, and the row-wise sparsity, i.e., the sparsity for each row of a given layer’s matrix,

maximizing the *neuron alignment* between dense and sparse activations. Contrary to OWL, NEURONAL does not require the user to specify any hyperparameter, as it automatically selects the most-performing values from a suitable set, hence adapting to the underlying model and the desired sparsity. Moreover, the use of alignment overcomes the necessity to define outliers on the activations, as done in OWL, which requires defining a threshold *a priori*. Finally, it does not use any gradient information [18, 45], hence significantly saving computational resources.

We test our approach on 3 Language Modeling datasets and 7 Zero-Shot tasks over 4 different LLM families from 7B to 13B parameters, to show its ability to outperform the most recent state-of-the-art techniques, including OWL [46] and DsNoT [49], over 3 different high sparsity values (60%, 70%, and 80%). To assess the robustness of our approach, we also conduct an in-depth ablation study.

2 Related Work

In this section, we provide a comprehensive discussion about network pruning applied to LLMs. We first introduce structured and unstructured network pruning; then, we focus on the latter, introducing the latest approaches proposed for improving sparse model performance.

Structured Network Pruning. Given a layer’s weight matrix $W \in \mathbb{R}^{n \times m}$ to sparsify, structured pruning removes either entire rows (n) or columns (m) (see the next section) aiming at speeding up both training and inference time. The first approach that applies structured pruning to LLMs has been proposed in [28], and focuses on the dependency of Transformers, i.e., it removes components of the networks while maximizing their original functionality. In [24], a pruning mechanism has been devised to remove components with the worst balance between loss and runtime. Other structured pruning approaches have been proposed based on combinatorial optimization [30], perturbative forward-pass only [9], and reduction of the embedding dimension through PCA [1]. Finally, in [17] it has been found that the last Transformer blocks are redundant, hence they can be completely removed with minor performance drops. The reason behind this phenomenon lies in the similarity between the learnable representation of consecutive blocks, which turns out to increase when the block depth increases. While all these approaches can achieve valuable inference speed-ups, the performance of the resulting sparse models w.r.t. their dense counterparts can be matched only at low sparsity values, such as 20% in [28] or 30% in [1]. This somehow limits the applicability of these methods, since in the case of models with billions of parameters one may need more aggressive pruning strategies to meet stringent hardware requirements.

Unstructured Network Pruning. Differently from structure pruning, unstructured pruning works by removing weights in a scattered (i.e., non-structured) way. While in this scenario the inference speed-up is limited (although techniques for reordering weights are available [26, 34, 50]), the performance w.r.t. the dense model can be preserved also at high sparsity ratios (i.e., above 50%), with the performance at lower sparsity being almost always completely preserved. The first approach of this kind has been proposed in [15], where weight pruning and reconstruction are combined based on the Hessian matrix. Even a simple magnitude-based approach turned out to perform well [21], as well when integrated with information on the neuron activations [40, 12]. All these approaches work by computing a score for each weight and then removing, uniformly for each layer, the worst-performing ones for a given sparsity ratio.

Top-Up Algorithms To improve the performance of unstructured pruning algorithms, several *top-up* algorithms have been devised. These approaches can be categorized into two distinct groups: methods that minimize the reconstruction error keeping the sparsity uniform for each block, and methods that modify the block-wise sparsity of the model resulting in non-uniform sparsity distribution across blocks.

The first group firstly sparsifies the model using a pruning algorithm and then, either dynamically [49] or by backpropagation [18], updates the pruning mask. The second group (to which our method belongs) modifies the block-wise sparsity (obtained by a given pruning algorithm) based either on activations’ outliers [46] or on layer-wise sparsity using block-wise reconstruction error with gradient information [45].

The idea of simply redistributing the layer-wise sparsity is known to be extremely well-performing on Multi-Layer Perceptrons (MLPs) and Convolutional Neural Networks (CNNs). The first approach of this kind, based on the Erdős–Rényi (ER) model, has been proposed in [35] for MLPs and then adjusted for CNNs in [11], while an empirical study about the effect of layer-wise pruning using different sparsity ratios has been done in [27]. Regarding Transformers (both for vision and text), the state-of-the-art algorithms [15, 40] have been devised to set the block-wise sparsity across the Transformer blocks in a uniform way. Later on, OWL has been proposed to build upon scoring-based pruning algorithms, adjusting the block-wise sparsity in a non-uniform way w.r.t. the number of outliers computed for each block. This approach improves the performance of several pruning algorithms, e.g. [15, 40], especially at sparsity above 60%. On the same line, BESA [45] allocates layer-wise sparsity across each block’s layer using gradient information. Recently, modality-wise sparsity distribution has been investigated in the case of multimodal tasks in [12, 19].

3 Observational Study

As discussed earlier, OWL [46] uses a non-uniform sparsity distribution across blocks, which provides an advantage in terms of performance w.r.t. uniform distribution. However, the reason why this occurs remains unclear. In the first part of this section, we focus on uncovering the reason behind this phenomenon. Furthermore, OWL suffers from some disadvantages: it requires the setting of two hyperparameters, one for the sparsity difference between consecutive blocks to utilize in the non-uniform distribution (λ), and one for the outlier definition (M). In the second part of this section, we investigate how the choice of the best hyperparameters is tied to the model and sparsity selected. This limitation leads to either selecting non-optimal hyperparameters or requiring a grid search to find the optimal values.

The observational study has been performed on two models (Phi-2 and LLama-1 7B) and three different sparsity ratios (0.6, 0.7, 0.8) using as pruning algorithm both Wanda [40] and MULTIFLOW [12]¹.

3.1 ① Non-Uniform Block-Wise Sparsity Distribution

We start by analyzing if the OWL’s performance improvement, compared to uniform sparsity distribution, could be *unequivocally* associated with its outlier-based score. Since the number of outliers for each block turns out to decrease with the layer depth, we test three straightforward non-uniform sparsity schedules (namely *linear*, *exponential*, and *logarithmic*), which do not require any forward step and do not depend on the outliers. Given a fixed parameter λ , these schedules work by redistributing the sparsity across layers in a monotonically increasing way (i.e., the sparsity of layer i is always larger than the sparsity of layer $i - 1$, $\forall i > 1$). Fig. 1 displays the improvement, w.r.t. uniform distribution, achieved by the three sparsity schedules on two pruning algorithms (Wanda and MULTIFLOW) with $\lambda = 0.08$ (as in [46]). The results highlight how non-uniform sparsity schedules, with no outlier information, can match, and in some cases even improve, the performance of OWL. Overall, the linear schedule turns out to be the most reliable one since it does not show oscillations in performance across the different sparsity ratios (while this happens for the logarithmic and exponential schedule).

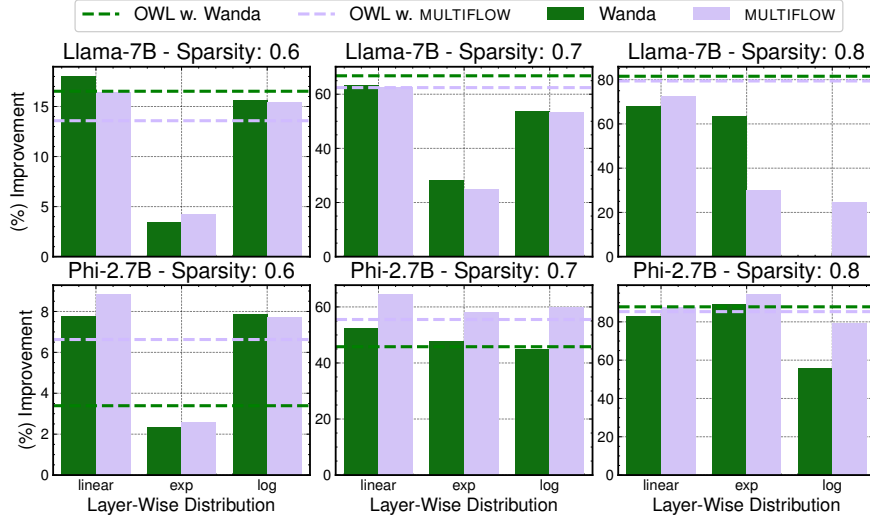


Figure 1: Average perplexity improvement (percentage) w.r.t. uniform distribution, computed over 3 Language Modeling datasets when applying non-uniform distribution with linear, exponential, and logarithmic schedules. The horizontal dashed lines refer to the improvement w.r.t. uniform distribution achieved by OWL when applied to each of the two base pruning algorithms.

3.2 ② Effect of λ and M

We then analyze the effect of the two hyperparameters set by OWL, namely λ and M . The first hyperparameter is used to set how much the sparsity can vary across blocks (i.e., $[s - \lambda, s + \lambda]$) while keeping the overall sparsity fixed as s . In the experimentation reported in [46], λ is set differently for each model, with 0.08 being the most used value. As

¹We did not include BESA [45] since it requires gradient information and works layer-based rather than block-based. We consider only *gradient-free* state-of-the-art methods.

a matter of fact, we found that this value is not effective with all models and sparsity ratios. We test OWL, applied again to Wanda and MULTIFLOW, with 12 different values of λ , and computed the perplexity on the 3 Language Modeling datasets. As we show in Figure 2, it turns out that OWL achieves the best results for each model-sparsity combination for different values of λ , which suggests the difficulty of setting this hyperparameter *a priori*. The second hyperparameter, M , defines the outliers' threshold: namely, for each block, the number of outliers is computed as the number of activations that are M times greater than the block's activations' mean. We replicated the same analysis carried out for λ and also for M , testing 12 different values on the 3 Language Modeling datasets when applying OWL to Wanda and MULTIFLOW. As for λ , we found that the optimal setting of M heavily depends on the model and sparsity (noting that in [46] the most used value is 5), as depicted in Figure 3.

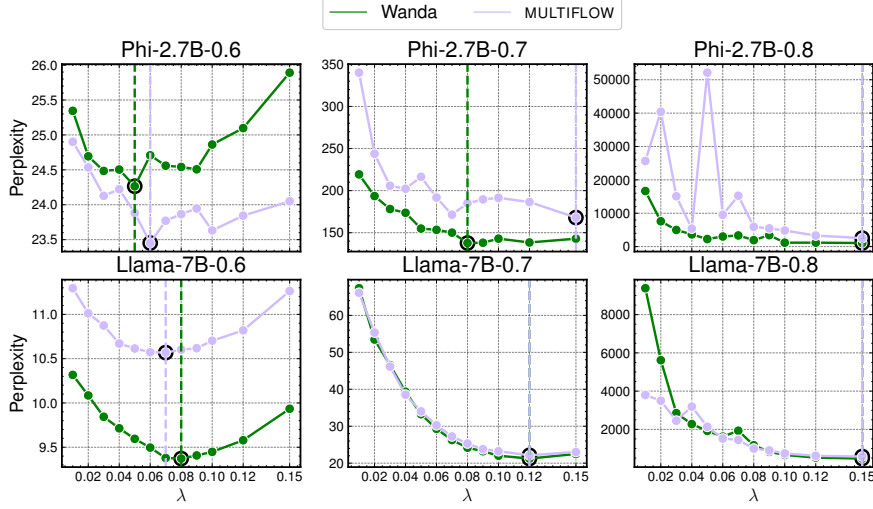


Figure 2: Perplexity for different values of λ over WikiText2 using OWL's non-uniform distribution across blocks.

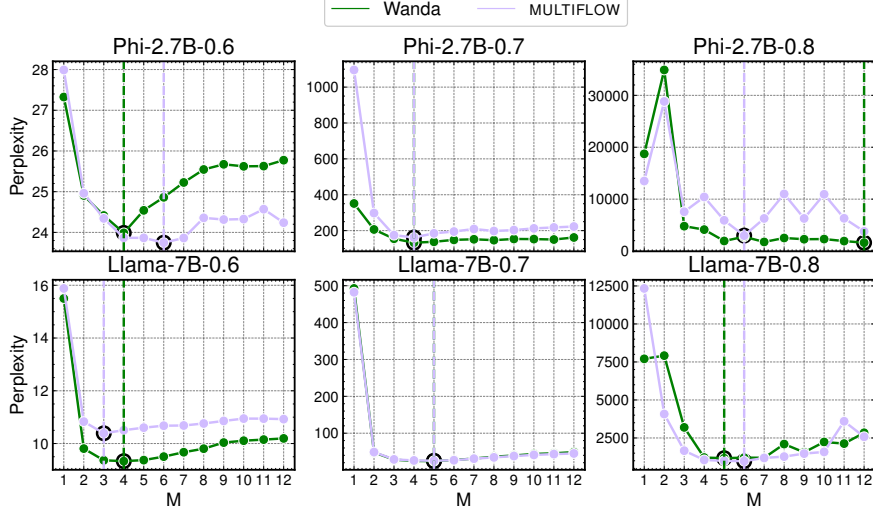


Figure 3: Perplexity for different values of M over WikiText2 using $\lambda = 0.08$.

To summarize, in ① we found that even if the non-uniform sparsity distribution proposed in OWL leads to better performance w.r.t. uniform distribution, this improvement is not entirely based on the outliers' distribution. Instead, a simple increase of the block-wise sparsity across the layer depths can explain the performance improvement. In ②, we showed how the performance of OWL is heavily sensitive to the choice of λ and M . In the next section, we will present our method to address this OWL's limitation.

4 Methodology

In this section, we propose our method, NEURONAL (Neuron Alignment). Given a pruning algorithm for a pre-trained LLM, our method re-computes the block-wise sparsity ratios for each Transformer block and the row-wise sparsity ratios based on the alignment between the dense activations and the sparse activations. The main strength of this method lies in its ability to be fully *adaptive* to the model and desired sparsity (given as input), requiring no single hyperparameter to be chosen *a priori*, but rather a set of suitable values from which NEURONAL can pick the most performing one.

Preliminaries Given a dense model \mathcal{D} , a pruning algorithm \mathcal{P} , and a desired sparsity s , unstructured network pruning generally computes a saliency score Ψ for each weight $w \in \mathcal{D}$ and then binarizes these scores w.r.t. the top_k elements, where $k = 1 - |\mathcal{D}| \times s$. This allows to obtain a binary mask \mathcal{M} to apply over \mathcal{D} , from which the final sparse model can be computed as $\mathcal{S} = \mathcal{D} \odot \mathcal{M}$. Since LLMs are composed of stacked Transformer blocks (each one denoted as \mathcal{B}_i), i.e., sets of linear layers (each one denoted as ℓ_i^j) that implement the self-attention mechanism followed by an MLP, the binarization step is usually done uniformly per each layer ℓ_i^j [15, 40] as:

$$\mathcal{M}^{\ell_i^j} = \text{top}_{k^{\ell_i^j}}(\Psi^{\ell_i^j}, \mathcal{D}^{\ell_i^j}). \quad (1)$$

Neuron Alignment Our proposed method is based on the idea of combining the concept of *neuron alignment*, which requires no *a priori* definition of outliers (hence no M parameter, as in OWL), with that of *adaptivity*, to remove the dependence from λ . Differently from the well-established reconstruction error [15], computed as $\arg \min_{M_\ell, W_\ell} \|W_\ell X_\ell - (M_\ell \odot W_\ell) X_\ell\|_2^2$ for each layer or block (hence measuring the difference between the sparse and dense representation of the output prior the non-linearity functions), *neuron alignment* provides a single scalar value that evaluates the model in its completeness focusing on the difference between sparse and dense activations, hence after the non-linearity. The method takes as input both \mathcal{D} and its sparse version \mathcal{S} generated by \mathcal{P} with sparsity ratio s , and uses a small calibration data C_λ to make a forward pass on both models, to retrieve the dense and sparse activations, respectively $\mathcal{A}_\mathcal{D}$ and $\mathcal{A}_\mathcal{S}$. The main idea behind NEURONAL is to maximize the neuron alignment by firstly modifying the vector of sparsity ratios for all blocks (\mathbf{s}^B) and then for all rows (\mathbf{s}^r), where each row corresponds to the layer's weight matrix $W^{\ell_i^j}$ (for each layer ℓ_i^j in \mathcal{B}_i), where $W^{\ell_i^j} \in \mathbb{R}^{r \times m}$. The main strength of this approach is that it does not require any weight update nor gradient information, but just a block- and row-wise recalibration and mask update via Eq. (1), using the same scoring criteria of \mathcal{P} .

However, as tested in the previous observational study, finding the best block/row-wise sparsity requires defining a factor λ to control the block/row-wise sparsity difference between consecutive blocks/rows while ensuring the desired global sparsity. As seen earlier, while OWL requires λ to be set *a priori*, we design NEURONAL to automatically select, from a suitable set of values, the best λ for each combination of \mathcal{D} , \mathcal{P} and s , yielding an adaptive top-up method. The only constraint we set is that we use a linear sparsity schedule over λ for the block-wise step, demonstrated to be effective in our observational study ①. This choice has been made (1) because we found that the performance improvement obtained with the linear sparsity schedule is more stable, see Fig. 1, and (2) to align our method to the latest research that shows how the last layers of an LLM have a small influence on the final performance [17, 29].

4.1 Block-Wise Sparsity Ratio

The first step concerns the block-wise redistribution over the whole model. Our method takes as input the dense and sparse models (\mathcal{D} and \mathcal{S}), the desired sparsity ratio (s), the calibration data C_λ , and a set of different λ parameters (λ^{set}). Then, it computes a set of $|\lambda^{\text{set}}|$ different vectors of block-wise sparsity values for the whole model $\mathbf{s}_{\text{set}}^B = \{\mathbf{s}_{\lambda_1}^B, \mathbf{s}_{\lambda_2}^B, \dots, \mathbf{s}_{\lambda_{|\lambda^{\text{set}}|}}^B\}$, where each element $\mathbf{s}_{\lambda_k}^B$ indicates a vector of block-wise sparsity values obtained with a linear schedule in $[s - \lambda_k, s + \lambda_k]$. For each $\mathbf{s}_{\lambda_k}^B$, we then forward the calibration data C_λ through the model, and calculate the corresponding neuron alignment:

$$neur_{al} = \sum_{\mathcal{B}_i} \sum_{\ell_i^j} \frac{\left\| \tilde{A}_D^j - \tilde{A}_{\mathcal{S}(\mathbf{s}_{\lambda_k}^B)}^j \right\|_2}{|\tilde{A}_D^j|} \quad (2)$$

where \tilde{A} means that the activations are normalized to sum up to one. Then, we select $(\mathbf{s}_{\text{set}}^B)^*$, i.e., the λ parameters per block that minimize Eq. (2). Finally, we update the block-wise sparsity with the selected $(\mathbf{s}_{\text{set}}^B)^*$ via Eq. (1), thus obtaining a sparsified model \mathcal{S}_B .

4.2 Row-Wise Sparsity Ratio

The second step is complementary to the previous one, but in this case, the sparsity is modified w.r.t. the rows of each layer. It is established [40] that pruning using the row as a *comparison group*² achieves better performance w.r.t. using the whole layer since it inherently maximizes the network connectivity [20, 7]. Here, we rely on such discovery to strengthen our approach and change the row-wise sparsity based on the neuron alignment of each layer. In this case, for each layer ℓ_i^j (i.e., for each $W^{\ell_i^j} \in \mathbb{R}^{r \times m}$) we redistribute the sparsity across the r rows. Also in this case the λ parameters are critical for deciding how to control the sparsity difference between consecutive rows. We take our sparse model obtained with the block-wise redistribution (\mathcal{S}_B) and, for each layer ℓ_i^j , we compute different row-wise sparsity values obtaining $\mathbf{s}_{set}^s = \{\mathbf{s}_{\lambda_1}^r, \mathbf{s}_{\lambda_2}^r, \dots, \mathbf{s}_{\lambda_{|\lambda_{set}|}}^r\}$, where each $\mathbf{s}_{\lambda_k}^r$ indicates a vector of row-wise sparsity ranging in $[s - \lambda_k, s + \lambda_k]$, where each element is inversely proportional to the alignment of the corresponding row. In this case, we select in \mathbf{s}_{set}^s the row-wise vector $(\mathbf{s}_{set}^s)^*$ that minimizes Eq. (2), and then apply Eq. (1) to \mathcal{S}_B , using each row as comparison group.

The full procedure composed of both the block-wise and row-wise recalibration is summarized in Algorithm 1.

Algorithm 1 Proposed top-up pruning procedure

```

Require:  $\mathcal{D}, \mathcal{P}, s, C_\lambda, \lambda_{set}$ 
 $\mathcal{M} \leftarrow \mathcal{P}(\mathcal{D}, s)$ 
 $\mathcal{S} \leftarrow \mathcal{D} \odot \mathcal{M}$  ▷ Prune  $\mathcal{D}$  uniformly per layer
 $A_{\mathcal{D}} \leftarrow \mathcal{D}(C_\lambda)$  ▷ Dense activations
 $(\mathbf{s}_{set}^B)^* \leftarrow \text{NEURONAL}(\mathcal{D}, \mathcal{S}, \lambda_{set}, C_\lambda, A_{\mathcal{D}})$  ▷ Block-wise step
 $\mathcal{S}_B \leftarrow \mathcal{D} \odot \text{top}_{(\mathbf{s}_{set}^B)^*}(\Psi, \mathcal{D})$ 
 $(\mathbf{s}_{set}^r)^* \leftarrow \text{NEURONAL}(\mathcal{D}, \mathcal{S}_B, \lambda_{set}, C_\lambda, A_{\mathcal{D}})$  ▷ Row-wise step
 $\mathcal{S}_{\text{final}} \leftarrow \mathcal{D} \odot \text{top}_{(\mathbf{s}_{set}^r)^*}(\Psi, \mathcal{D})$ 

function  $\text{NEURONAL}(\mathcal{D}, \mathcal{S}, s, \lambda_{set}, C_\lambda, A_{\mathcal{D}})$ 
     $\mathbf{s}^* \leftarrow \emptyset, \text{neur}_{al}^* \leftarrow \infty$ 
    for  $\lambda \in \lambda_{set}$  do
         $\mathbf{s}_\lambda = \text{GETDIST}(s, \lambda)$  ▷ Compute  $\mathbf{s}_\lambda^B$  or  $\mathbf{s}_\lambda^r$ 
         $A_{\mathcal{S}} \leftarrow (\mathcal{D} \odot \text{top}_{\mathbf{s}_\lambda}(\Psi, \mathcal{D}))(C_\lambda)$  ▷ Sparse activations
         $\text{neur}_{al} \leftarrow \text{GETALIGN}(A_{\mathcal{D}}, A_{\mathcal{S}}, \mathbf{s}_\lambda)$  ▷ Via Eq. (2)
        if  $\text{neur}_{al} < \text{neur}_{al}^*$  then
             $\mathbf{s}^* \leftarrow \mathbf{s}_\lambda$ 
    return  $\mathbf{s}^*$ 

```

5 Experiments

We apply our proposed NEURONAL to different pruning algorithms tailored for LLMs. Specifically, we test how it compares in terms of performance over Language Modeling datasets and Zero-Shot tasks w.r.t. the most recent top-up algorithms for pruning. We also perform scalability and ablation studies to show the effectiveness of our NEURONAL.

5.1 Experimental Setup

Language Modeling Datasets To measure the models’ perplexity on Language Modeling datasets, we use the following three datasets: (1) **WikiText2** [31], a collection of $2.6M$ tokens from Wikipedia; (2) Colossal Clean Common Crawl (**C4**) [37], which is a clean version of the Common Crawl dataset produced in April 2019, containing $154G$ tokens [10]; and (3) Penn Treebank (**PTB**), which is a dataset extracted from the Wall Street Journal containing $2.4M$ tokens.

Zero-Shot Tasks To assess more thoroughly how the different pruning algorithms affect the models’ capabilities, we employ the following 7 datasets. (1) Recognizing Textual Entailment (**RTE**) [8, 2, 16, 3], a dataset composed of 3000 test samples in which a model has to detect the entailment between two sentences. (2) **Winogrande** [23], a dataset consisting of 1767 test cases in which the model has to fill a blank using two choices. (3) **BoolQ** [5], a question-answering dataset containing 3270 test samples, where each question requires a yes/no answer. (4) **HellaSwag** [47], a dataset composed of $10k$ test cases that requires a model to select the appropriate completion for a given sentence

²Here, *comparison group* refers to the subset of weights whose scores are compared to decide which weights to prune.

Table 1: Perplexity on the 3 Language Modeling datasets computed over 5 different LLMs for four different top-up algorithms (Uniform, DSnoT, OWL, and NEURONAL) on 3 pruning algorithms (Magnitude, MULTIFLOW, and Wanda) at 70% sparsity.

Algorithm	Top-Up	Phi-2.7B			LLama-1 7B			LLama-2 7B			Mistral 7B			OPT 6.7B		
		WikiText2	C4	PTB	WikiText2	C4	PTB	WikiText2	C4	PTB	WikiText2	C4	PTB	WikiText2	C4	PTB
Magnitude	Uniform	764.6	384.4	983.9	2.53e4	2.25e4	3.26e4	1.42e5	1.02e4	2.02e6	221.9	232.9	748.7	1.00e4	5.39e3	6.54e3
	DSnoT	539.0	258.0	656.2	1.02e7	2.77e6	4.99e7	1.31e8	2.90e7	2.25e8	192.7	189.7	566.2	6.16e3	3.93e3	4.36e3
	OWL	419.6	242.7	358.5	1.20e4	6.58e3	5.39e4	3.39e5	1.24e4	3.28e6	111.7	124.2	545.5	1.57e4	8.48e3	9.67e3
	NEURONAL	278.6	177.0	316.0	208.7	203.8	3.70e3	155.8	264.8	2.61e3	46.1	42.7	552.7	2.10e4	1.07e4	1.09e4
MULTIFLOW	Uniform	388.4	298.8	610.8	80.9	71.9	172.4	60.0	58.8	1260.4	936.8	656.3	2062.5	943.6	1250.4	843.1
	DSnoT	325.5	261.9	328.8	67.6	65.0	114.7	66.6	75.8	688.9	57.4	63.3	264.8	241.8	153.3	263.9
	OWL	197.9	141.3	293.9	25.1	25.8	78.9	29.2	31.0	547.1	329.0	764.3	1718.2	240.9	495.6	337.8
	NEURONAL	110.7	91.0	192.0	20.6	21.2	45.9	22.0	23.8	265.5	197.2	343.9	954.0	221.7	86.5	219.7
Wanda	Uniform	227.6	182.7	346.2	85.1	86.2	157.0	78.0	81.0	599.3	60.7	73.6	298.3	157.5	260.1	209.2
	DSnoT	221.9	172.6	257.6	72.9	76.0	121.0	76.1	85.7	491.8	81.3	79.9	304.8	191.4	173.3	182.6
	OWL	132.7	116.2	183.7	24.6	27.3	61.2	30.5	36.6	333.7	41.0	51.8	253.5	54.4	69.7	100.7
	NEURONAL	89.9	78.9	133.9	21.5	23.2	43.8	23.9	27.2	205.3	28.9	33.9	197.8	183.9	87.3	194.7

from a set of possibilities. (5) **ARC-e** [6], the “easy” fold from the AI2 Reasoning Challenge, containing 2376 questions with multiple-choice answers. (6) **ARC-c** [6], the “challenge” fold from the AI2 Reasoning Challenge, containing 1172 questions that were not solvable for methods that perform well on the ARC-e dataset. (7) **OBQA** [32], a dataset containing 500 test multiple-choice questions about core science facts, asked in novel contexts.

Baselines As pruning algorithms, we test Magnitude, MULTIFLOW [12], and Wanda [40]. All are tested with three different top-up algorithms (besides ours): (1) **Uniform** distribution, (2) **DSnoT** [49] (dynamic training-free uniform distribution with mask update), and (3) **OWL** [46] (block-wise training-free non-uniform distribution based on outliers scores). All these baselines are tested considering as comparison group each row: in other words, for a given layer, the sparsity s is uniform for each row of each matrix rather than uniform across matrices. This is done for two main reasons: 1) as mentioned earlier, it is established that row-wise pruning on LLMs leads to better performance w.r.t. layer-wise pruning [40], and 2) since our approach relies on a row-wise step, for fairness we also use row as comparison group (rather than layer) on all the other methods, to appreciate the benefit of our approach. We also test our approach, as well as the baselines, on SparseGPT [15], using in this case only the block-wise approach, since SparseGPT relies on a weight reconstruction mechanism that firstly prunes columns and then updates the rows of the pruned cells, which makes it unfeasible to apply our row-wise approach. The results on SparseGPT can be found in Tables 14-16 in the Appendix. For all the pruning algorithms that use calibration data (i.e., MULTIFLOW, Wanda, and SparseGPT), we use 128 samples from the C4 dataset, as in [15, 40].

Models and Sparsity Since one of the main distinctive features of NEURONAL is its ability to adapt to sparsity and models, we test 4 different LLM families. Specifically, we evaluate **LLama-7B** (both V1 and V2) [41, 42], **Phi-2**, **Mistral-7B** [22], and **OPT-6.7B** [48]. To scale up the models’ size, we also test LLama-13 (both V1 and V2). In the paper, we mainly present results at 70% sparsity, for fair comparisons with [46]. However, to assess the generalization to different sparsity ratios we also include 60% and 80% sparsity in our experiments, see the Appendix for details.

NEURONAL Setup Our proposed method works by taking as input an LLM model, a desired sparsity ratio, a scoring-based pruning algorithm, and two sets of λ parameters (one for the block-wise and one for the row-wise steps). In our experiments, we gave as input $\lambda^{\text{set}} \in [0.01, 0.02, 0.03, 0.05, 0.06, 0.07, 0.08, 0.09, 0.1, 0.12, 0.15, 0.20, 0.25]$ for the block-wise step, while for the row-wise step we also added 0.0 (in case of no performance improvement). Each value in λ^{set} has been evaluated (as described in Algorithm 1) over a calibration data C_λ . Since all the base pruning algorithms require a single forward over C (where $|C| = 128$) sequences with 2048 tokens each, while OWL requires a second forward always over C , to make the computational runtime similar we set $C_\lambda = 8$ (the closest power of 2 w.r.t. $|C|/|\lambda^{\text{set}}|^3$). Doing so, the computational time required by NEURONAL is only two forward steps more than the base pruning algorithms, and one forward more than OWL⁴. All the experiments have been run on NVIDIA A100 GPUs, both with 40 and 80 GB.

5.2 Experimental Results

Concerning the Language Modeling datasets, the numerical results in terms of perplexity computed over the 3 Language Modeling datasets at 70% sparsity are shown in Table 1. It can be seen how NEURONAL is able in almost all cases to outperform all the other baselines by a large margin. In no case NEURONAL performs worse w.r.t. the uniform

³In Fig. 11 in the Appendix we report the results with different sizes of C_λ , showing how NEURONAL is robust to $|C_\lambda|$.

⁴For both C and C_λ , we use the same seed (0) for the calibration set, i.e., C_λ contains the first 8 elements of C .

Table 2: Zero-Shot accuracy for 7 tasks, computed over 5 different LLMs for 3 different top-up pruning algorithms (DSnoT, OWL, and NEURONAL) on two pruning algorithms (MULTIFLOW and Wanda) at 70% sparsity. “Average” indicates the mean accuracy across tasks. The rows corresponding to the pruning algorithms refer to uniform distribution.

Model	Algorithm	RTE	WinoGrande	BoolQ	HellaSwag	ARC-e	ARC-c	OBQA	Average
Phi-2.7B	MULTIFLOW	53.79	50.43	53.49	28.43	46.59	20.48	15.6	38.40
	w. DSnoT	52.71	54.06	54.92	28.38	44.15	21.5	15.6	38.76
	w. OWL	52.35	55.33	61.99	30.31	54.59	24.23	18.4	42.46
	w. NEURONAL	53.07	58.01	62.17	33.33	51.52	25.43	17.6	43.02
	Wanda	52.35	53.2	62.14	28.31	44.87	20.99	17.4	39.89
	w. DSnoT	52.35	51.54	60.98	28.33	41.62	21.08	15.4	38.76
	w. OWL	52.71	53.59	62.05	30.09	48.61	22.53	18.8	41.20
	w. NEURONAL	52.71	58.01	62.17	32.37	49.62	22.95	17.2	42.15
	MULTIFLOW	55.96	52.57	61.96	29.77	34.64	19.45	15.2	38.51
	w. DSnoT	54.15	50.43	59.33	29.33	36.45	19.28	13.6	37.51
Llama1 7B	w. OWL	52.35	58.64	62.63	36.74	47.43	26.62	18.2	43.23
	w. NEURONAL	58.12	61.33	63.55	38.23	50.76	26.71	22.6	45.90
	Wanda	55.23	52.8	57.46	28.84	32.2	18.0	13.8	36.90
	w. DSnoT	54.15	51.22	54.56	28.97	33.08	18.26	13.6	36.26
	w. OWL	58.48	58.56	62.60	34.74	47.35	24.06	17.4	43.31
	w. NEURONAL	54.51	58.72	63.30	37.06	49.92	26.37	20.6	44.35
Llama2 7B	MULTIFLOW	52.71	50.99	62.05	28.52	33.04	17.92	13.6	36.98
	w. DSnoT	52.71	50.99	59.72	27.92	32.58	16.81	13.0	36.25
	w. OWL	52.71	56.12	62.05	32.40	42.42	19.88	18.6	40.60
	w. NEURONAL	54.15	58.09	62.42	35.29	48.36	22.53	21.2	43.15
	Wanda	52.71	48.46	49.94	28.09	30.39	19.2	11.8	34.37
	w. DSnoT	52.71	50.36	47.77	27.67	30.6	17.32	12.2	34.09
	w. OWL	52.71	55.96	62.11	31.86	43.73	20.65	17.0	40.57
	w. NEURONAL	52.71	57.62	62.72	35.47	50.25	22.01	20.6	43.05
Mistral-7B	MULTIFLOW	49.82	50.75	41.19	26.45	26.64	21.84	12.6	32.76
	w. DSnoT	52.71	52.57	62.42	29.51	36.66	18.94	12.0	37.83
	w. OWL	53.79	49.17	38.90	26.77	27.78	19.20	12.8	32.63
	w. NEURONAL	52.35	50.83	37.98	27.24	27.74	18.34	13.8	32.61
	Wanda	52.71	51.62	59.79	28.86	34.18	18.17	12.6	36.85
	w. DSnoT	52.71	50.28	58.62	28.51	33.54	18.86	13.2	36.53
	w. OWL	52.71	53.91	62.20	30.95	39.39	18.60	13.6	38.77
	w. NEURONAL	52.71	60.22	62.20	34.69	44.32	20.73	15.6	41.50
OPT-6.7B	MULTIFLOW	53.79	49.72	43.0	26.48	30.51	20.05	13.8	33.91
	w. DSnoT	53.79	49.01	61.1	27.01	32.87	18.34	12.2	36.33
	w. OWL	48.74	48.62	61.56	27.18	35.69	16.47	11.6	35.69
	w. NEURONAL	49.10	50.43	62.17	31.37	40.28	22.01	17.0	38.91
	Wanda	52.71	49.72	60.03	26.91	35.86	17.75	11.2	36.31
	w. DSnoT	52.71	49.57	60.61	26.91	35.06	17.58	12.0	36.35
	w. OWL	53.79	51.22	61.87	29.53	42.3	18.09	14.6	38.77
	w. NEURONAL	50.90	51.30	62.17	30.68	39.77	21.76	14.6	38.74

distribution. The only model on which NEURONAL is not the best top-up algorithm for all pruning algorithms is OPT. In all other cases, NEURONAL outperforms OWL for all models and pruning algorithms. The results at 60% and 80% sparsity shown in Tables 6-7 in the Appendix confirm this trend.

As for the Zero-Shot tasks, the numerical results are shown in Table 2⁵. Again, NEURONAL turns out to outperform in the majority of cases all the baselines. In 8 cases out of 10 (w.r.t. the mean accuracy across all tasks), NEURONAL is the one that reaches the best performance. The results for 60% and 80% sparsity are available in Tables 8-9 in the Appendix, where we observe a similar trend.

Scalability Study To assess if the NEURONAL performance scales to bigger models, we apply it to Llama-13B (both V1 and V2) on the Language Modeling datasets. The results available in Table 3 (top) show how our approach is even more effective with larger models. For the 70% sparsity ratio, NEURONAL turns out to reach the best performance over both models, for all pruning algorithms. Impressively, the gap in performance w.r.t. the other baselines (in

⁵Magnitude is removed from this table due to space constraints. Its results are available separately in Tables 10-12 in the Appendix.

Table 3: Perplexity of LLama-13B on the 3 Language Modeling datasets at 70% (top) and 80% sparsity (bottom).

Algorithm	Top-Up	Llama-1 13B			Llama-2 13B		
		WikiText2	C4	PTB	WikiText2	C4	PTB
Magnitude	Uniform	5610.6	3682.9	20040.0	191.0	159.1	2784.1
	DSnoT	7420.1	2264.0	48325.4	121.7	103.0	2331.2
	OWL	279.4	438.9	11502.2	33.3	35.4	1267.2
	NEURONAL	55.4	83.3	841.1	45.2	44.4	321.1
MULTIFLOW	Uniform	49.4	45.3	277.8	144.3	112.4	623.2
	DSnoT	46.2	48.9	240.4	45.8	54.2	611.5
	OWL	16.6	17.7	132.2	54.0	56.2	426.6
	NEURONAL	13.7	15.4	98.7	17.3	20.0	275.2
Wanda	Uniform	54.4	55.3	309.2	45.7	56.2	571.0
	DSnoT	47.8	54.2	248.6	46.6	57.7	555.5
	OWL	16.3	18.9	147.6	18.0	21.8	315.1
	NEURONAL	14.3	16.6	85.4	16.5	19.3	239.6
Magnitude	Uniform	26696.2	26319.4	27180.9	12020.1	11161.9	10210.6
	DSnoT	5591.8	4131.3	5732.3	5822.9	6510.2	10668.0
	OWL	21985.6	19564.4	24511.7	5208.2	5058.5	10202.2
	NEURONAL	133.4	183.8	1727.7	574.3	386.2	4169.1
MULTIFLOW	Uniform	3711.2	1696.1	3588.4	4481.2	2409.8	5209.6
	DSnoT	5368.4	2863.6	6286.3	1943.3	1669.5	5279.7
	OWL	813.8	375.7	2138.8	1802.3	1012.2	4394.9
	NEURONAL	61.8	65.7	414.9	323.1	259.6	1301.6
Wanda	Uniform	3479.3	1959.8	3566.1	1124.6	870.5	5549.8
	DSnoT	43684.1	24432.2	32162.1	4441.2	3957.9	4092.8
	OWL	761.6	368.1	1929.8	248.0	204.2	2027.1
	NEURONAL	64.0	68.5	413.8	116.5	103.2	814.8

particular uniform distribution) is even more marked than in the smaller models tested previously. The improvement of NEURONAL over the baselines is even more evident at 80% sparsity, see Table 3 (bottom), where in several cases it outperforms OWL by 1-2 orders of magnitude. This is confirmed also at 60% sparsity, see Table 13 in the Appendix.

NEURONAL vs block-only vs row-only Since NEURONAL is based on two consecutive steps (for brevity, we call them here *block* and *row*), we test the performance of the *block* and *row* steps applied alone. This means that in the *block*-only setting the sparsity of each block one is given by our NEURONAL, while the row-wise sparsity for each layer is fixed to s . Instead, for the *row*-only setting, the sparsity for each block is fixed at s , while the row-wise sparsity for each layer is given by our neuron alignment mechanism. Table 4 shows the results of such ablation. The results confirm that NEURONAL (with both steps) achieves better performance in most of the cases, although this depends on the sparsity ratio (at lower sparsity, the *block*-only setting is the best one in 3 out of 5 cases). It is worth noticing that in such cases the gap w.r.t. NEURONAL is marginal and that NEURONAL always outperforms the uniform distribution. However, on high sparsity NEURONAL always performs best, with a large margin w.r.t. the second best (which is always the *block*-only setting). It is also clear how most of the performance improvement of NEURONAL comes from the *block* step, while the *row* step yields a moderate improvement, which however increases when increasing the sparsity ratio.

NEURONAL λ Selection In this section, we report an analysis of the ability of NEURONAL to pick the best λ parameters (i.e., the parameters for which the performance is the best one, hence the lowest value if computed over perplexity). To do this, we evaluate NEURONAL for all the λ parameters (in the *block*-only scenario to simplify the visualization of results) over the 3 Language Modeling datasets. Fig. 4 reports the perplexity at 70% sparsity across different values of λ (black dots connected by solid lines), while the dots highlighted in orange indicate the perplexity achieved with the λ value selected by NEURONAL. These results highlight how NEURONAL, in the majority of the cases, can pick the optimal value of λ both with data knowledge, as in the C4 dataset (from which the calibration data is sampled), as well as on unseen datasets such as WikiText2 and PTB. Fig.s 9-10 in the Appendix show the results at 60%-80% sparsity.

Calibration Data Since NEURONAL works by finding the best λ parameters w.r.t. to the neuron alignment using a calibration sample of 8 samples, we test the results under different seeds for the calibration data. The results in Table 5 show the mean and standard deviation of perplexity at 70% sparsity over the 3 Language Modeling datasets (see

Table 4: Ablation study: perplexity achieved when using the *block* and *row* steps alone over the C4 dataset.

Sparsity	Top-Up	Model				
		Phi-2.7B	LLama1 7B	LLama2 7B	Mistral-7B	OPT-6.7B
60%	Uniform	29.3	13.7	14.0	15.9	17.9
	NEURONAL <i>block</i> -only	27.3	11.8	11.9	13.8	17.8
	NEURONAL <i>row</i> -only	29.2	14.0	14.5	15.9	19.7
70%	NEURONAL	27.2	12.0	12.0	13.8	19.1
	Uniform	182.7	86.2	81.0	73.6	260.1
	NEURONAL <i>block</i> -only	82.0	22.4	25.6	35.4	91.4
80%	NEURONAL <i>row</i> -only	175.6	85.4	88.9	73.6	152.0
	NEURONAL	78.9	23.2	27.2	34.0	87.3
	Uniform	12422.9	3969.8	3117.3	277.7	2345.8
80%	NEURONAL <i>block</i> -only	3177.3	296.2	313.8	181.8	530.6
	NEURONAL <i>row</i> -only	16501.8	4597.5	824.9	277.7	2345.8
	NEURONAL	2404.5	242.0	226.2	168.6	471.4

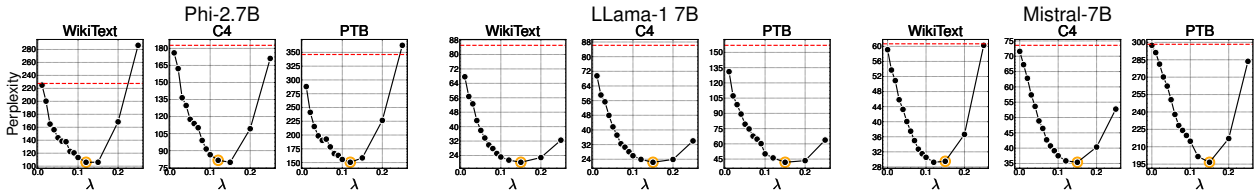


Figure 4: Perplexity over different values of λ at 70% sparsity. The orange dot indicates the value selected by NEURONAL. The best λ is retrieved by maximizing the neuron alignment computed over C_λ on the C4 dataset, and then it is transferred to the other datasets. The red line corresponds to the perplexity using a uniform distribution, hence $\lambda = 0$.

Tables 19-20 in the Appendix for the same ablation at 60% and 80% sparsity). It is visible how the standard deviation is minimal w.r.t. the mean, apart from the OPT model where the standard deviation turns out to be higher. This dependence on the calibration data could explain the reason why, as discussed before, our proposed approach works better than the baselines on all other models but struggles with the OPT family. The ablation on the number of samples (see Fig. 11 in the Appendix) supports this hypothesis. In fact, OPT models are the only ones to show performance oscillation depending on the calibration data seed and especially the number of samples, which does not happen with all the other LLM families.

Table 5: Ablation study: perplexity achieved when using NEURONAL with different calibration data seeds (0, 16, 46) at 70% sparsity over the 3 Language Modeling datasets.

Dataset	Model				
	Phi-2.7B	LLama1 7B	LLama2 7B	Mistral-7B	OPT-6.7B
WikiText2	85.5 ± 3.3	22.7 ± 2.1	23.6 ± 0.2	29.0 ± 0.1	137.4 ± 71.2
C4	76.3 ± 2.2	24.2 ± 1.5	27.0 ± 0.2	34.2 ± 0.3	75.9 ± 16.2
PTB	135.8 ± 4.8	46.5 ± 5.0	200.4 ± 3.6	205.0 ± 6.7	154.5 ± 63.6

6 Conclusion and Limitations

In this paper, we proposed NEURONAL, a new approach to prune LLMs based on the alignment between sparse and dense activations. Our approach has the main strength of requiring no outliers or gradient information. On top of that, our method is also adaptive, since it is designed to automatically select the best hyperparameters for the model, pruning algorithm, and desired sparsity. Throughout extensive experiments, we showed how our approach outperforms all the latest state-of-the-art methods both on Language Modeling datasets and Zero-Shot tasks, on 4 different LLM families and 3 sparsity ratios. We also included an extensive ablation study to show the robustness of our approach to the calibration data as well as the effect of its algorithmic steps.

In our view, the present version of NEURONAL has three main limitations. (1) With NEURONAL, it is not possible to make use of optimized structured-sparsity inference implementations (e.g, the NVIDIA N:M sparsity [36]): for a given sparsity, NEURONAL produces customized sparsity constraints for each layer in a block, and then for each row of each layer. Therefore, these implementations cannot be employed as they often require continuity in the sparsity of matrices. (2) NEURONAL requires two forward steps more than base pruning algorithms, and one more than the closest top-up competitor, OWL. (3) Finally, it requires the definition of λ^{set} . However, it is worth noticing that $|\lambda^{\text{set}}|$ as well as $|\mathcal{C}_\lambda|$ affect the computational cost of the forward step.

References

- [1] Saleh Ashkboos, Maximilian L Croci, Marcelo Gennari do Nascimento, Torsten Hoefer, and James Hensman. SliceGPT: Compress Large Language Models by Deleting Rows and Columns. In *International Conference on Learning Representations*, 2023.
- [2] Roy Bar Haim, Ido Dagan, Bill Dolan, Lisa Ferro, Danilo Giampiccolo, Bernardo Magnini, and Idan Szpektor. The second PASCAL recognising textual entailment challenge, 2006.
- [3] Luisa Bentivogli, Ido Dagan, Hoa Trang Dang, Danilo Giampiccolo, and Bernardo Magnini. The fifth PASCAL recognizing textual entailment challenge. In *Text Analysis Conference*, 2009.
- [4] Yupeng Chang, Xu Wang, Jindong Wang, Yuan Wu, Linyi Yang, Kaijie Zhu, Hao Chen, Xiaoyuan Yi, Cunxiang Wang, Yidong Wang, et al. A survey on evaluation of large language models. *ACM Transactions on Intelligent Systems and Technology*, 15(3):1–45, 2024.
- [5] Christopher Clark, Kenton Lee, Ming-Wei Chang, Tom Kwiatkowski, Michael Collins, and Kristina Toutanova. BoolQ: Exploring the Surprising Difficulty of Natural Yes/No Questions. In *Conference of the North American Chapter of the Association for Computational Linguistics: Human Language Technologies, Volume 1 (Long and Short Papers)*, pages 2924–2936, 2019.
- [6] Peter Clark, Isaac Cowhey, Oren Etzioni, Tushar Khot, Ashish Sabharwal, Carissa Schoenick, and Oyvind Tafjord. Think you have Solved Question Answering? Try ARC, the AI2 Reasoning Challenge. *arXiv preprint arXiv:1803.05457v1*, 2018.
- [7] Elia Cunegatti, Matteo Farina, Doina Bucur, and Giovanni Iacca. Understanding Sparse Neural Networks from their Topology via Multipartite Graph Representations. *Transactions on Machine Learning Research*, 2024.
- [8] Ido Dagan, Oren Glickman, and Bernardo Magnini. The PASCAL recognising textual entailment challenge. In *Machine learning challenges. Evaluating predictive uncertainty, Visual object classification, and Recognizing textual entailment*, pages 177–190. Springer, 2006.
- [9] Lucio Dery, Steven Kolawole, Jean-Francois Kagey, Virginia Smith, Graham Neubig, and Ameet Talwalkar. Everybody Prune Now: Structured Pruning of LLMs with only Forward Passes. *arXiv preprint arXiv:2402.05406*, 2024.
- [10] Jesse Dodge, Maarten Sap, Ana Marasović, William Agnew, Gabriel Ilharco, Dirk Groeneveld, Margaret Mitchell, and Matt Gardner. Documenting Large Webtext Corpora: A Case Study on the Colossal Clean Crawled Corpus. In *Conference on Empirical Methods in Natural Language Processing*, pages 1286–1305, 2021.
- [11] Utku Evci, Trevor Gale, Jacob Menick, Pablo Samuel Castro, and Erich Elsen. Rigging the lottery: Making all tickets winners. In *International Conference on Machine Learning*, pages 2943–2952. PMLR, 2020.
- [12] Matteo Farina, Massimiliano Mancini, Elia Cunegatti, Gaowen Liu, Giovanni Iacca, and Elisa Ricci. MULTIFLOW: Shifting Towards Task-Agnostic Vision-Language Pruning. In *IEEE/CVF Conference on Computer Vision and Pattern Recognition*, pages 16185–16195, 2024.
- [13] Jonathan Frankle and Michael Carbin. The lottery ticket hypothesis: Finding sparse, trainable neural networks. *arXiv preprint arXiv:1803.03635*, 2018.
- [14] Jonathan Frankle, Gintare Karolina Dziugaite, Daniel Roy, and Michael Carbin. Pruning neural networks at initialization: Why are we missing the mark? In *International Conference on Learning Representations*, 2020.
- [15] Elias Frantar and Dan Alistarh. SparseGPT: Massive language models can be accurately pruned in one-shot. In *International Conference on Machine Learning*, pages 10323–10337. PMLR, 2023.
- [16] Danilo Giampiccolo, Bernardo Magnini, Ido Dagan, and Bill Dolan. The third PASCAL recognizing textual entailment challenge. In *ACL-PASCAL workshop on textual entailment and paraphrasing*, pages 1–9. Association for Computational Linguistics, 2007.

[17] Andrey Gromov, Kushal Tirumala, Hassan Shapourian, Paolo Glorioso, and Daniel A Roberts. The unreasonable ineffectiveness of the deeper layers. *arXiv preprint arXiv:2403.17887*, 2024.

[18] Song Guo, Fan Wu, Lei Zhang, Xiawu Zheng, Shengchuan Zhang, Fei Chao, Yiyu Shi, and Rongrong Ji. EBFT: Effective and Block-Wise Fine-Tuning for Sparse LLMs. *arXiv preprint arXiv:2402.12419*, 2024.

[19] Shuai He and Tianlong Chen. RESSA: Repair Sparse Vision-Language Models via Sparse Cross-Modality Adaptation. *arXiv preprint arXiv:2404.02424*, 2024.

[20] Duc NM Hoang and Shiwei Liu. Revisiting pruning at initialization through the lens of Ramanujan graph. In *International Conference on Learning Representations*, 2023.

[21] Ajay Jaiswal, Shiwei Liu, Tianlong Chen, Zhangyang Wang, et al. The emergence of essential sparsity in large pre-trained models: The weights that matter. *Advances in Neural Information Processing Systems*, 36, 2024.

[22] Albert Q Jiang, Alexandre Sablayrolles, Arthur Mensch, Chris Bamford, Devendra Singh Chaplot, Diego de las Casas, Florian Bressand, Gianna Lengyel, Guillaume Lample, Lucile Saulnier, et al. Mistral 7B. *arXiv preprint arXiv:2310.06825*, 2023.

[23] Sakaguchi Keisuke, Le Bras Ronan, Bhagavatula Chandra, and Choi Yejin. WinoGrande: An Adversarial Winograd Schema Challenge at Scale. *arXiv preprint arXiv:1907.10641*, 2019.

[24] Eldar Kurtić, Elias Frantar, and Dan Alistarh. ZipLM: Inference-Aware Structured Pruning of Language Models. *Advances in Neural Information Processing Systems*, 36, 2024.

[25] Namhoon Lee, Thalaiyasingam Ajanthan, and Philip HS Torr. Snip: Single-shot network pruning based on connection sensitivity. *arXiv preprint arXiv:1810.02340*, 2018.

[26] Jiajia Li, Bora Uçar, Ümit V Çatalyürek, Jimeng Sun, Kevin Barker, and Richard Vuduc. Efficient and effective sparse tensor reordering. In *ACM International Conference on Supercomputing*, pages 227–237, 2019.

[27] Shiwei Liu, Tianlong Chen, Xiaohan Chen, Li Shen, Decebal Constantin Mocanu, Zhangyang Wang, and Mykola Pechenizkiy. The unreasonable effectiveness of random pruning: Return of the most naive baseline for sparse training. In *International Conference on Learning Representations*, 2021.

[28] Xinyin Ma, Gongfan Fang, and Xinchao Wang. LLM-pruner: On the structural pruning of large language models. *Advances in Neural Information Processing Systems*, 36, 2023.

[29] Xin Men, Mingyu Xu, Qingyu Zhang, Bingning Wang, Hongyu Lin, Yaojie Lu, Xianpei Han, and Weipeng Chen. ShortGPT: Layers in large language models are more redundant than you expect. *arXiv preprint arXiv:2403.03853*, 2024.

[30] Xiang Meng, Shibal Ibrahim, Kayhan Behdin, Hussein Hazimeh, Natalia Ponomareva, and Rahul Mazumder. OSSCAR: One-Shot Structured Pruning in Vision and Language Models with Combinatorial Optimization. *arXiv preprint arXiv:2403.12983*, 2024.

[31] Stephen Merity, Caiming Xiong, James Bradbury, and Richard Socher. Pointer sentinel mixture models. *arXiv preprint arXiv:1609.07843*, 2016.

[32] Todor Mihaylov, Peter Clark, Tushar Khot, and Ashish Sabharwal. Can a suit of armor conduct electricity? a new dataset for open book question answering. *arXiv preprint arXiv:1809.02789*, 2018.

[33] Bonan Min, Hayley Ross, Elior Sulem, Amir Pouran Ben Veyeh, Thien Huu Nguyen, Oscar Sainz, Eneko Agirre, Ilana Heintz, and Dan Roth. Recent advances in natural language processing via large pre-trained language models: A survey. *ACM Computing Surveys*, 56(2):1–40, 2023.

[34] Asit Mishra, Jorge Albericio Latorre, Jeff Pool, Darko Stosic, Dusan Stosic, Ganesh Venkatesh, Chong Yu, and Paulius Micikevicius. Accelerating sparse deep neural networks. *arXiv preprint arXiv:2104.08378*, 2021.

[35] Decebal Constantin Mocanu, Elena Mocanu, Peter Stone, Phuong H Nguyen, Madeleine Gibescu, and Antonio Liotta. Scalable training of artificial neural networks with adaptive sparse connectivity inspired by network science. *Nature Communications*, 9(1):2383, 2018.

[36] Jeff Pool. Accelerating sparsity in the nvidia ampere architecture. *GTC 2020*, 2020.

[37] Colin Raffel, Noam Shazeer, Adam Roberts, Katherine Lee, Sharan Narang, Michael Matena, Yanqi Zhou, Wei Li, and Peter J Liu. Exploring the limits of transfer learning with a unified text-to-text transformer. *Journal of Machine Learning Research*, 21(140):1–67, 2020.

[38] Jingtong Su, Yihang Chen, Tianle Cai, Tianhao Wu, Ruiqi Gao, Liwei Wang, and Jason D Lee. Sanity-checking pruning methods: Random tickets can win the jackpot. *Advances in Neural Information Processing Systems*, 33, 2020.

- [39] Mingjie Sun, Xinlei Chen, J Zico Kolter, and Zhuang Liu. Massive activations in large language models. *arXiv preprint arXiv:2402.17762*, 2024.
- [40] Mingjie Sun, Zhuang Liu, Anna Bair, and J Zico Kolter. A simple and effective pruning approach for large language models. In *International Conference on Learning Representations*, 2023.
- [41] Hugo Touvron, Louis Martin, Kevin Stone, Peter Albert, Amjad Almahairi, Yasmine Babaei, Nikolay Bashlykov, Soumya Batra, Prajjwal Bhargava, Shruti Bhosale, et al. Llama 2: Open foundation and fine-tuned chat models. *arXiv preprint arXiv:2307.09288*, 2023.
- [42] Hugo Touvron, Louis Martin, Kevin Stone, Peter Albert, Amjad Almahairi, Yasmine Babaei, Nikolay Bashlykov, Soumya Batra, Prajjwal Bhargava, Shruti Bhosale, et al. Llama 2: Open foundation and fine-tuned chat models. *arXiv preprint arXiv:2307.09288*, 2023.
- [43] Chaoqi Wang, Guodong Zhang, and Roger Grosse. Picking winning tickets before training by preserving gradient flow. *arXiv preprint arXiv:2002.07376*, 2020.
- [44] Jason Wei, Xuezhi Wang, Dale Schuurmans, Maarten Bosma, Fei Xia, Ed Chi, Quoc V Le, Denny Zhou, et al. Chain-of-thought prompting elicits reasoning in large language models. *Advances in Neural Information Processing Systems*, 35:24824–24837, 2022.
- [45] Peng Xu, Wenqi Shao, Mengzhao Chen, Shitao Tang, Kaipeng Zhang, Peng Gao, Fengwei An, Yu Qiao, and Ping Luo. BESA: Pruning large language models with blockwise parameter-efficient sparsity allocation. In *International Conference on Learning Representations*, 2024.
- [46] Lu Yin, You Wu, Zhenyu Zhang, Cheng-Yu Hsieh, Yaqing Wang, Yiling Jia, Gen Li, AJAY KUMAR JAISWAL, Mykola Pechenizkiy, Yi Liang, Michael Bendersky, Zhangyang Wang, and Shiwei Liu. Outlier weighed layerwise sparsity (OWL): A missing secret sauce for pruning LLMs to high sparsity. In *International Conference on Machine Learning*. PMLR, 2024.
- [47] Rowan Zellers, Ari Holtzman, Yonatan Bisk, Ali Farhadi, and Yejin Choi. HellaSwag: Can a Machine Really Finish Your Sentence? In *Annual Meeting of the Association for Computational Linguistics*, pages 4791–4800, 2019.
- [48] Susan Zhang, Stephen Roller, Naman Goyal, Mikel Artetxe, Moya Chen, Shuohui Chen, Christopher Dewan, Mona Diab, Xian Li, Xi Victoria Lin, et al. OPT: Open Pre-trained Transformer Language Models. *arXiv preprint arXiv:2205.01068*, 2022.
- [49] Yuxin Zhang, Lirui Zhao, Mingbao Lin, Sun Yunyun, Yiwu Yao, Xingjia Han, Jared Tanner, Shiwei Liu, and Rongrong Ji. Dynamic sparse no training: Training-free fine-tuning for sparse LLMs. In *International Conference on Learning Representations*, 2024.
- [50] Aojun Zhou, Yukun Ma, Junnan Zhu, Jianbo Liu, Zhijie Zhang, Kun Yuan, Wenxiu Sun, and Hongsheng Li. Learning N:M Fine-grained Structured Sparse Neural Networks From Scratch. In *International Conference on Learning Representations*, 2021.

A Appendix

A.1 Observational Study

Here we include the results of the observational study on the OWL’s hyperparameters λ and M computed on the C4 dataset (Fig.s 5 and 7), and PTB (Fig.s 6 and 8). The results confirm the findings presented in the main text: there is no single hyperparameter selection (both M and λ) that reaches the best performance across all different model-pruning-sparsity settings.

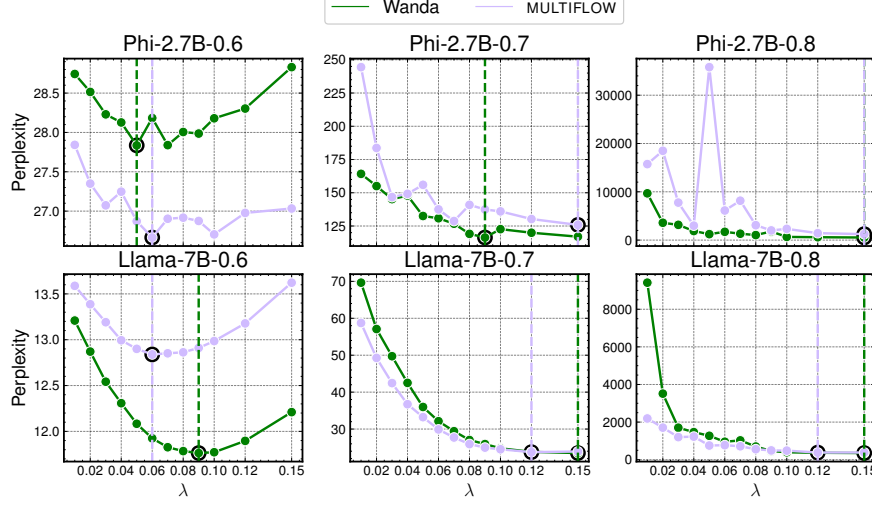


Figure 5: Perplexity for different λ values over C4 using OWL’s non-uniform distribution across blocks.

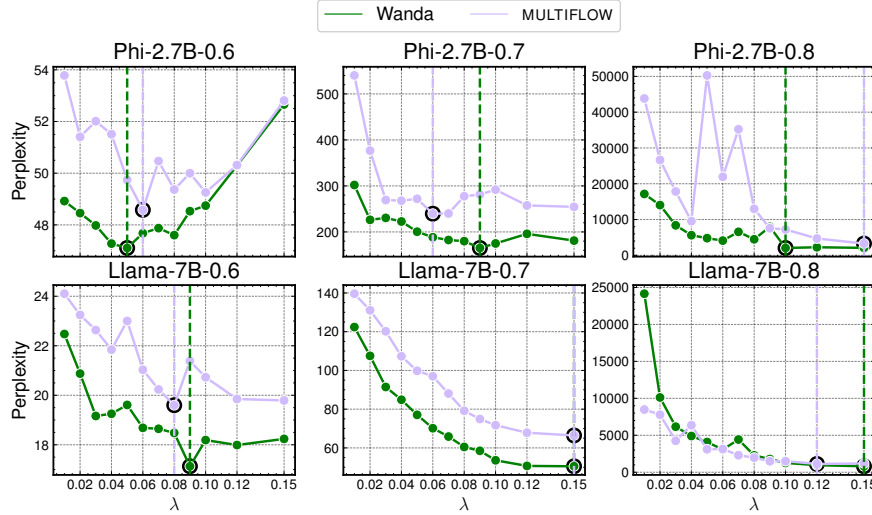


Figure 6: Perplexity for different λ values over PTB using OWL’s non-uniform distribution across blocks.

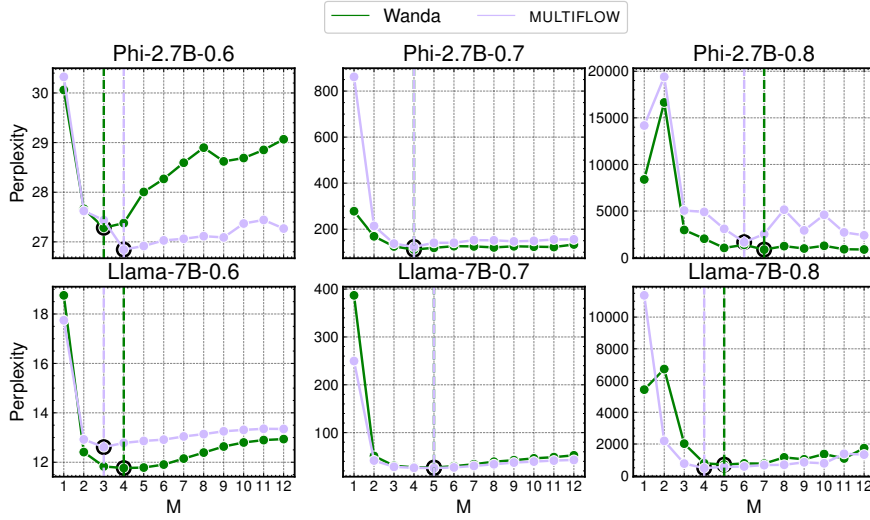


Figure 7: Perplexity for different M values over C4 using $\lambda = 0.08$.

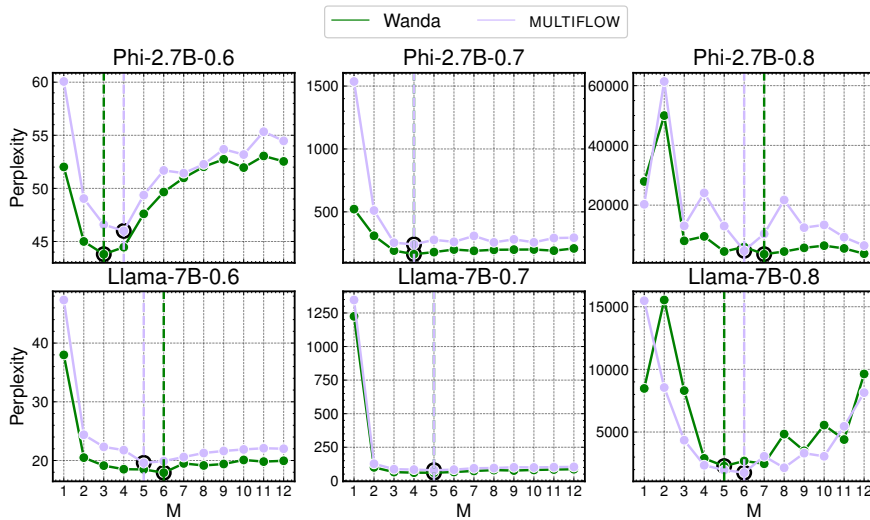


Figure 8: Perplexity for different M values over PTB using $\lambda = 0.08$.

A.2 Additional Experiments

Here we include the results of the experiments that, due to space limits, we could not include in the main text. Specifically, we report: the results of NEURONAL over Language Modeling and Zero-Shot tasks at 60% and 80% sparsity; the results for the Zero-Shot tasks with Magnitude pruning; the results over LLama-13B at 70% sparsity; the results of NEURONAL (*block*-only) applied to SparseGPT [15].

A.2.1 Language Modeling at 60% and 80% sparsity

In Table 6-7, we report the results of NEURONAL over the 3 Language Modeling datasets (WikiText2, C4, and PTB) with the five different models considered in the main text, for 60% and 80% sparsity. In the first case, our approach turns out to be the best one in 23 out of 45 cases, while for 80% sparsity in 27 out of 45. It is interesting to notice how at medium sparsity (60%) all the top-up algorithms, including ours, provide similar results, while the improvement provided by NEURONAL at 80% (w.r.t. the top-up competitors) in some cases reaches a factor 5x (e.g., with Llama-1 7B for MULTIFLOW and Wanda).

Table 6: Perplexity on the 3 Language Modeling datasets computed over 5 different LLMs for four different top-up algorithms (Uniform, DSnoT, OWL, and NEURONAL) on 3 pruning algorithms (Magnitude, MULTIFLOW, and Wanda) at 60% sparsity.

Algorithm	Top-Up	Phi-2.7B			LLama-1 7B			LLama-2 7B			Mistral 7B			OPT 6.7B		
		WikiText2	C4	PTB	WikiText2	C4	PTB	WikiText2	C4	PTB	WikiText2	C4	PTB	WikiText2	C4	PTB
Magnitude	Uniform	51.3	45.9	66.9	152.4	159.8	3016.1	6894.8	42666.8	1706134.9	19.6	24.4	189.3	9489.3	6203.7	6759.1
	DSnoT	55.9	48.9	64.1	131.6	114.7	1460.3	3676.6	67845.5	7299247.0	15.3	19.6	146.2	8077.8	6062.6	6948.2
	OWL	46.5	42.2	65.7	50.5	62.9	249.4	810.9	19356.5	2302446.2	12.0	15.8	169.1	6811.7	3666.8	4065.4
	NEURONAL	48.6	44.9	65.1	55.8	63.6	153.1	52.4	79.3	24807.9	12.6	17.2	123.9	1212.3	551.4	935.0
MULTIFLOW	Uniform	25.4	28.3	54.7	11.6	13.9	26.0	11.0	13.7	166.9	167.7	341.0	884.3	16.3	19.7	26.8
	DSnoT	37.2	42.1	50.2	10.1	12.7	18.2	10.5	13.4	137.6	10.9	14.8	86.0	15.9	19.2	25.3
	OWL	23.8	26.7	49.8	10.6	12.9	19.6	10.1	12.7	106.0	84.1	123.0	644.6	16.1	18.5	25.5
	NEURONAL	23.7	27.0	42.5	9.9	12.2	17.6	9.8	12.2	72.3	86.1	140.3	562.3	17.0	20.4	28.1
Wanda	Uniform	225.8	29.3	48.9	10.7	13.7	24.0	10.8	14.0	122.2	11.3	15.9	101.6	15.2	17.9	23.7
	DSnoT	32.2	38.0	50.6	10.4	13.2	20.8	10.8	14.1	109.6	11.4	15.9	96.8	15.8	19.1	24.6
	OWL	24.8	28.2	48.6	9.4	11.8	18.5	9.2	11.9	75.1	10.3	14.5	84.5	15.7	17.8	24.5
	NEURONAL	25.2	27.2	42.1	9.6	12.0	17.4	9.4	12.0	65.1	9.9	13.8	74.6	16.3	19.1	25.2

Table 7: Perplexity on the 3 Language Modeling datasets computed over 5 different LLMs for four different top-up algorithms (Uniform, DSnoT, OWL, and NEURONAL) on 3 pruning algorithms (Magnitude, MULTIFLOW, and Wanda) at 80% sparsity.

Algorithm	Top-Up	Phi-2.7B			LLama-1 7B			LLama-2 7B			Mistral 7B			OPT 6.7B		
		WikiText2	C4	PTB	WikiText2	C4	PTB	WikiText2	C4	PTB	WikiText2	C4	PTB	WikiText2	C4	PTB
Magnitude	Uniform	15320.0	17856.3	31988.6	112885.2	113922.4	139627.3	55800.7	52597.2	89843.5	24815.2	31186.7	7984.1	42902.5	21284.4	22110.8
	DSnoT	19977.5	20700.7	18369.5	33994.8	34213.5	72003.2	2358414.2	1802890.0	3015785.0	13297.5	8025.4	5804.0	18112.4	11853.1	14438.1
	OWL	6625.1	5597.4	8388.0	169148.8	158523.1	134038.4	26898.0	17892.9	57863.3	9614.4	8503.8	5789.5	33174.7	17756.7	21613.0
	NEURONAL	10193.9	9578.7	14227.3	82221.7	85688.7	108410.1	92725.2	67827.9	104616.8	2188.8	1205.3	3226.2	30303.8	20846.6	16807.1
MULTIFLOW	Uniform	25257.3	12842.4	25929.7	4829.9	2307.4	9806.2	2037.9	1464.8	3878.2	4289.7	2976.3	3812.4	4422.8	2382.7	3276.9
	DSnoT	8498.5	3918.3	12343.8	3697.1	2649.8	8263.4	1721.1	1543.0	3443.8	327.0	270.0	752.5	11633.7	9715.6	11764.5
	OWL	6255.2	2798.5	13600.8	926.5	563.1	1783.4	544.2	414.3	2819.3	3354.5	2209.7	3555.2	13461.5	11133.9	15080.8
	NEURONAL	3550.3	1279.8	5411.4	311.6	188.4	564.8	230.2	269.8	2355.9	983.1	617.5	1467.4	1118.7	591.5	1173.3
Wanda	Uniform	20498.5	12422.9	31362.6	5219.5	3969.8	10013.6	4929.7	3117.3	5285.2	330.9	277.7	783.7	4259.6	2345.8	2732.1
	DSnoT	15269.0	6855.4	14008.5	3709.7	3076.0	7790.7	5199.4	4443.2	6685.7	346.5	277.3	758.4	7754.1	6157.5	7779.7
	OWL	2546.5	1209.5	7061.7	986.5	654.5	2000.4	663.0	486.2	2283.4	206.3	187.8	603.9	13190.1	10605.6	14228.5
	NEURONAL	3873.6	2404.5	6675.9	376.1	242.0	566.3	213.9	226.2	993.2	226.3	168.6	698.2	988.2	471.4	988.7

A.2.2 Zero-Shot at 60% and 80% sparsity

In Tables 8-9, we report the results at 60% and 80% sparsity of NEURONAL over Zero-Shot tasks with the five different models tested in the main text. In the first case, our approach turns out to be the best one (when considering the average over the 7 tasks) in 7 out of 10 cases, while for 80% sparsity in 8 out of 10. This further validates the results presented in the main text (for 70% sparsity) since it shows the ability of NEURONAL to provide stable and consistent results over more complicated tasks at different (and high) sparsity levels.

Table 8: Zero-Shot accuracy for 7 tasks, computed over 5 different LLMs for 3 different top-up pruning algorithms (DSnoT, OWL, and NEURONAL) on two pruning algorithms (MULTIFLOW and Wanda) at 60% sparsity. “Average” indicates the mean accuracy across tasks. The rows corresponding to the pruning algorithms refer to uniform distribution.

Model	Algorithm	RTE	Winograde	BoolQ	HellaSwag	ARC-e	ARC-c	OBQA	Average
Phi-2.7B	MULTIFLOW	62.09	67.64	63.15	42.04	71.76	39.51	27.2	53.34
	w. DSnoT	63.18	66.77	43.49	40.84	66.62	35.41	26.0	48.90
	w. OWL	64.62	67.17	60.15	41.78	70.96	37.8	28.8	53.04
	w. NEURONAL	62.09	67.40	67.22	42.73	71.04	38.65	27.6	53.82
	Wanda	63.54	64.8	69.08	40.16	68.64	34.9	25.4	52.36
	w. DSnoT	62.45	64.33	59.17	39.25	64.18	33.53	22.6	49.36
	w. OWL	64.62	64.33	64.83	39.80	67.63	34.98	24.2	51.48
	w. NEURONAL	63.54	67.09	67.74	40.51	66.54	34.04	24.4	51.98
	MULTIFLOW	57.04	62.51	67.19	45.31	59.55	30.97	24.6	49.60
Llama1 7B	w. DSnoT	49.46	63.06	68.32	44.75	63.80	31.23	26.4	49.57
	w. OWL	54.15	63.46	66.54	46.53	60.65	31.14	25.4	49.70
	w. NEURONAL	49.10	63.46	68.35	47.89	63.51	32.42	27.8	50.36
	Wanda	59.57	62.67	68.81	43.64	62.84	30.38	24.8	50.39
	w. DSnoT	51.62	61.64	67.37	43.39	63.89	30.55	25.4	49.12
Llama2 -7B	w. OWL	55.60	64.17	70.61	46.63	62.96	31.74	24.8	50.93
	w. NEURONAL	57.76	64.09	70.24	46.59	63.97	31.14	26.2	51.43
	MULTIFLOW	57.04	61.96	64.80	43.39	60.44	29.1	24.6	48.76
	w. DSnoT	54.15	63.77	63.91	43.42	66.25	31.83	24.0	49.62
	w. OWL	54.87	62.75	65.14	45.20	62.58	29.52	23.8	49.12
Mistral-7B	w. NEURONAL	52.71	65.90	69.51	46.60	65.87	31.66	24.8	51.01
	Wanda	54.15	64.48	65.44	43.85	65.19	30.46	26.2	49.97
	w. DSnoT	53.79	64.09	64.83	42.39	63.89	30.03	22.8	48.83
	w. OWL	53.79	66.61	66.76	46.63	67.63	32.34	28.0	51.68
	w. NEURONAL	53.07	66.06	70.46	46.93	66.67	31.74	26.8	51.68
OPT-6.7B	MULTIFLOW	51.62	49.88	39.17	27.49	29.67	18.77	11.0	32.51
	w. DSnoT	54.87	66.61	70.86	45.93	68.27	32.94	24.0	51.93
	w. OWL	53.07	50.12	46.33	28.29	32.58	19.28	13.2	34.70
	w. NEURONAL	52.71	52.49	52.97	28.77	33.42	18.43	13.2	36.00
	Wanda	54.87	66.06	71.13	44.48	67.05	32.00	21.60	51.03
OPT-6.7B	w. DSnoT	54.15	65.59	70.43	44.5	66.88	31.40	20.60	50.51
	w. OWL	57.04	67.17	73.85	45.66	67.89	32.59	23.20	52.49
	w. NEURONAL	56.32	65.82	70.70	46.71	67.63	33.36	23.20	51.96
	MULTIFLOW	52.71	58.25	62.69	42.24	56.52	25.68	22.20	45.76
	w. DSnoT	53.07	58.48	62.57	42.13	57.79	23.98	22.20	45.75
OPT-6.7B	w. OWL	53.07	57.46	63.21	42.98	56.44	25.68	24.20	46.15
	w. NEURONAL	52.71	58.64	62.17	41.83	56.31	25.09	22.20	45.56
	Wanda	52.71	59.67	62.29	42.80	58.00	25.60	22.6	46.24
	w. DSnoT	52.71	58.17	62.11	41.99	57.41	25.43	22.4	45.75
	w. OWL	52.71	58.72	62.69	42.14	58.33	25.17	22.6	46.05
OPT-6.7B	w. NEURONAL	52.71	61.25	62.29	42.00	57.49	25.43	23.0	46.31

Table 9: Zero-Shot accuracy for 7 tasks, computed over 5 different LLMs for 3 different top-up pruning algorithms (DSnoT, OWL, and NEURONAL) on two pruning algorithms (MULTIFLOW and Wanda) at 80% sparsity. “Average” indicates the mean accuracy across tasks. The rows corresponding to the pruning algorithms refer to uniform distribution.

Model	Algorithm	RTE	WinoGrande	BoolQ	HellaSwag	ARC-e	ARC-c	OBQA	Average
Phi-2.7B	MULTIFLOW	52.71	50.12	51.04	26.15	27.44	19.37	13.4	34.32
	w. DSnoT	50.18	49.49	37.83	26.32	27.82	19.97	13.8	32.2
	w. OWL	53.07	51.22	56.76	26.30	30.85	18.52	15.2	35.99
	w. NEURONAL	52.71	49.96	50.58	26.49	32.20	19.8	14.4	35.16
	Wanda	53.07	49.25	62.17	25.93	27.44	20.99	14.6	36.21
	w. DSnoT	53.07	50.99	38.04	26.17	27.10	20.73	13.0	32.73
	w. OWL	52.35	51.22	60.21	26.51	29.88	20.05	13.6	36.26
	w. NEURONAL	52.71	50.12	62.17	27.57	32.95	21.08	16.0	37.51
	MULTIFLOW	47.29	50.91	40.03	26.17	26.77	21.16	12.4	32.1
Llama-7B	w. DSnoT	46.57	50.43	37.83	26.02	27.06	20.05	12.2	31.45
	w. OWL	50.18	50.04	45.47	26.74	27.65	20.48	12.2	33.25
	w. NEURONAL	54.87	50.91	55.96	27.62	30.09	18.77	12.8	35.86
	Wanda	47.29	49.88	37.83	26.34	26.47	20.99	12.8	31.66
	w. DSnoT	46.93	50.36	37.83	26.03	26.56	21.33	13.4	31.78
	w. OWL	47.29	49.88	37.83	26.67	27.19	19.54	11.6	31.43
	w. NEURONAL	49.82	48.86	40.76	27.41	29.25	18.34	13.0	32.49
	MULTIFLOW	53.43	48.86	37.83	26.35	27.48	21.25	13.2	32.63
Llama2-7B	w. DSnoT	52.71	48.86	37.86	26.17	26.60	20.39	13.0	32.23
	w. OWL	52.71	49.49	37.83	26.62	26.94	19.11	12.6	32.19
	w. NEURONAL	52.71	50.36	44.74	27.47	28.62	17.58	14.4	33.70
	Wanda	47.65	49.41	37.83	25.82	26.52	20.82	14.6	31.81
	w. DSnoT	53.07	47.91	37.86	26.09	27.23	20.73	13.0	32.27
	w. OWL	52.71	50.83	37.83	26.52	27.27	19.37	12.8	32.48
	w. NEURONAL	52.71	49.49	37.89	27.38	28.58	17.58	14.8	32.63
	MULTIFLOW	50.18	48.15	37.80	25.67	26.18	22.70	13.20	31.98
Mistral-7B	w. DSnoT	52.71	47.36	37.83	26.58	28.03	18.94	13.8	32.18
	w. OWL	48.38	49.09	38.44	25.88	25.59	23.29	13.6	32.04
	w. NEURONAL	52.71	50.91	37.83	26.35	27.78	20.31	12.8	32.67
	Wanda	53.79	48.78	37.83	26.52	27.82	19.8	12.8	32.48
	w. DSnoT	52.35	48.30	37.83	26.55	27.44	19.54	13.0	32.14
	w. OWL	52.71	47.43	37.83	26.68	27.78	18.52	13.2	32.02
	w. NEURONAL	52.71	50.04	38.65	27.52	28.96	19.97	13.4	33.04
	MULTIFLOW	52.71	50.91	37.80	25.87	27.40	19.28	12.40	32.34
OPT-6.7B	w. DSnoT	52.71	50.83	57.31	26.00	25.00	20.22	11.80	34.84
	w. OWL	52.71	51.07	37.83	25.74	25.29	20.05	16.00	32.67
	w. NEURONAL	52.71	51.70	54.07	26.29	30.64	19.37	11.80	35.23
	Wanda	54.15	52.09	41.53	26.47	28.45	18.86	11.80	33.34
	w. DSnoT	52.71	51.38	55.32	26.17	27.06	19.37	13.80	35.12
	w. OWL	52.71	49.33	37.83	25.84	25.67	20.31	13.00	32.10
	w. NEURONAL	52.71	49.25	51.99	26.35	30.39	19.37	12.60	34.67

A.2.3 Zero-Shot at 60%, 70% and 80% sparsity with Magnitude

In Tables 10-12, we report the results of NEURONAL over Zero-Shot tasks using Magnitude pruning as the base pruning algorithm. The results provided by NEURONAL turn out to be the best ones in 9 out of 15 cases. It is also worth noticing that the performance gap between the Magnitude pruning and score-based pruning algorithms (such as Wanda or *multiflow*) is generally quite high. Hence, NEURONAL can improve the performance of Magnitude (in the standard setting with uniform distribution) to a certain degree since at high sparsity ratios (as the ones we test) the performance of Magnitude has been shown to be poor [21].

Table 10: Zero-Shot accuracy for 7 tasks, computed over 5 different LLMs for 3 different top-up pruning algorithms (DSnoT, OWL, and NEURONAL) on Magnitude at 60% sparsity. “Average” indicates the mean accuracy across tasks. The rows corresponding to the pruning algorithms refer to uniform distribution.

Model	Algorithm	RTE	Winogrande	BoolQ	HellaSwag	ARC-e	ARC-c	OBQA	Average
Phi-2.7B	Magnitude	57.04	62.83	51.38	42.56	66.33	35.41	28.2	49.11
	w. DSnoT	54.51	64.09	42.32	41.09	66.25	34.98	26.6	47.12
	w. OWL	55.23	62.59	48.81	42.53	67.38	38.48	28.4	49.06
	w. NEURONAL	54.15	65.19	47.28	42.36	65.95	36.77	26.8	48.36
Llama-7B	Magnitude	51.62	52.64	45.05	39.23	51.05	26.88	20.4	40.98
	w. DSnoT	52.35	52.80	46.88	38.3	50.59	26.37	20.6	41.13
	w. OWL	52.35	58.41	51.8	42.02	56.31	29.78	23.8	44.92
	w. NEURONAL	50.90	56.12	57.43	40.65	55.3	29.78	24.4	44.94
Llama2-7B	Magnitude	51.26	55.8	41.19	36.97	50.17	26.96	16.2	39.79
	w. DSnoT	53.79	56.04	42.87	38.3	53.28	27.9	19.8	41.71
	w. OWL	51.99	57.3	46.15	42.56	56.65	30.46	19.4	43.5
	w. NEURONAL	54.87	59.59	60.4	46.14	59.01	32.85	27.6	48.64
Mistral-7B	Magnitude	55.23	62.19	66.36	48.74	67.05	33.19	22.6	50.77
	w. DSnoT	55.6	62.35	68.53	48.28	67.51	33.11	23.2	51.23
	w. OWL	53.79	64.48	72.17	49.39	68.14	33.87	23.8	52.23
	w. NEURONAL	53.79	64.09	71.07	49.83	65.07	35.07	25.0	51.99
OPT-6.7B	Magnitude	53.43	50.59	37.86	26.38	26.6	21.42	13.2	32.78
	w. DSnoT	52.71	49.25	37.86	26.14	27.27	21.5	13.2	32.56
	w. OWL	52.71	50.51	37.83	26.77	30.3	18.52	14.8	33.06
	w. NEURONAL	52.71	54.22	39.14	33.3	37.71	24.23	16.8	36.87

Table 11: Zero-Shot accuracy for 7 tasks, computed over 5 different LLMs for 3 different top-up pruning algorithms (DSnoT, OWL, and NEURONAL) on Magnitude at 70% sparsity. “Average” indicates the mean accuracy across tasks. The rows corresponding to the pruning algorithms refer to uniform distribution.

Model	Algorithm	RTE	WinoGrande	BoolQ	HellaSwag	ARC-e	ARC-c	OBQA	Average
	Magnitude	46.93	53.59	47.22	30.45	47.85	24.57	19.2	38.54
Phi-2.7B	w. DSnoT	46.57	50.91	39.6	30.12	45.54	24.06	16.8	36.23
	w. OWL	45.13	52.88	49.2	32.26	51.64	27.56	21.4	40.01
	w. NEURONAL	47.65	53.51	54.25	33.4	53.7	29.61	20.6	41.82
	Magnitude	53.43	49.96	37.92	27.59	31.73	22.44	16.6	34.24
Llama-7B	w. DSnoT	52.71	51.7	37.83	27.71	30.26	22.7	15.4	34.04
	w. OWL	53.07	51.38	38.38	33.14	39.31	24.15	16.8	36.6
	w. NEURONAL	52.71	54.38	52.91	39.61	46.0	26.62	23.0	42.18
	Magnitude	51.26	49.96	37.86	25.9	28.45	23.12	13.4	32.85
Llama2 -7B	w. DSnoT	53.79	49.88	37.86	25.42	28.83	20.56	16.6	33.28
	w. OWL	53.07	50.28	37.89	26.38	30.77	22.7	15.0	33.73
	w. NEURONAL	54.51	55.41	64.86	33.25	42.09	27.47	21.2	42.68
	Magnitude	51.99	50.83	41.13	32.16	42.72	19.54	16.6	36.42
Mistral-7B	w. DSnoT	53.07	51.62	39.54	31.66	42.51	20.05	16.6	36.44
	w. OWL	57.76	56.59	49.17	36.48	45.75	22.01	18.8	40.94
	w. NEURONAL	53.79	57.54	62.72	38.68	44.11	26.45	20.6	43.41
	Magnitude	52.71	49.8	37.83	25.88	26.68	21.33	12.4	32.38
OPT-6.7B	w. DSnoT	52.71	49.96	37.83	25.87	27.19	20.14	13.6	32.47
	w. OWL	52.71	50.59	37.83	25.81	25.46	21.25	12.8	32.35
	w. NEURONAL	52.71	50.28	37.8	26.27	26.81	20.31	13.0	32.45

Table 12: Zero-Shot accuracy for 7 tasks, computed over 5 different LLMs for 3 different top-up pruning algorithms (DSnoT, OWL, and NEURONAL) on Magnitude at 80% sparsity. “Average” indicates the mean accuracy across tasks. The rows corresponding to the pruning algorithms refer to uniform distribution.

Model	Algorithm	RTE	WinoGrande	BoolQ	HellaSwag	ARC-e	ARC-c	OBQA	Average
	Magnitude	45.13	50.36	41.19	25.83	29.08	20.9	13.6	32.30
Phi-2.7B	w. DSnoT	46.93	52.33	39.63	25.9	28.32	21.25	13.4	32.54
	w. OWL	49.46	50.91	42.35	26.71	35.27	21.67	13.4	34.25
	w. NEURONAL	46.57	51.22	44.86	25.78	28.66	21.5	13.0	33.08
	Magnitude	46.21	49.96	53.98	25.69	24.83	21.84	13.8	33.76
Llama-7B	w. DSnoT	52.35	51.85	38.47	25.52	26.39	21.42	16.0	33.14
	w. OWL	48.38	48.93	44.74	25.76	26.35	21.08	15.8	33.01
	w. NEURONAL	47.29	48.86	50.34	25.82	26.18	21.25	14.6	33.48
	Magnitude	52.35	49.57	46.18	25.94	26.14	23.12	16.0	34.19
Llama2 -7B	w. DSnoT	52.71	51.54	37.89	25.46	27.10	22.44	15.4	33.22
	w. OWL	53.07	48.70	42.02	25.72	26.60	21.42	14.4	33.13
	w. NEURONAL	51.26	49.33	42.14	25.71	26.52	22.70	15.0	33.24
	Magnitude	51.26	50.99	41.16	25.93	27.48	21.84	14.6	33.32
Mistral-7B	w. DSnoT	52.35	49.72	38.07	26.26	26.43	21.25	14.0	32.58
	w. OWL	52.35	50.20	41.04	26.55	27.78	19.97	13.8	33.10
	w. NEURONAL	52.71	49.64	43.18	28.11	29.8	21.59	14.6	34.23
	Magnitude	52.71	49.49	37.83	25.79	26.39	21.25	13.0	32.35
OPT-6.7B	w. DSnoT	52.71	49.57	37.83	25.78	25.63	20.65	12.8	32.14
	w. OWL	52.71	49.80	37.83	26.05	26.73	21.16	13.2	32.50
	w. NEURONAL	52.71	51.78	37.83	25.79	26.89	21.08	12.8	32.70

A.2.4 NEURONAL on LLama-13B at 70% sparsity

In Table 13, we present the results on LLama-13B at 60% sparsity. The results are in line with the ones at 70% and 80% sparsity presented in the main text since NEURONAL can outperform the competitors in 11 out of 15 cases.

Table 13: Perplexity of LLama-13B on the 3 Language Modeling datasets at 60% sparsity.

Algorithm	Top-Up	Llama-1 13B			Llama-2 13B		
		WikiText2	C4	PTB	WikiText2	C4	PTB
Magnitude	Uniform	34.9	49.1	1413.7	10.1	13.3	457.5
	DSnoT	33.6	41.3	604.8	10.1	13.3	376.7
	OWL	28.5	36.6	255.0	8.9	11.6	217.2
	NEURONAL	24.8	35.1	186.9	9.5	12.3	151.1
MULTIFLOW	Uniform	8.7	10.9	66.5	16.3	21.0	211.6
	DSnoT	8.4	10.8	58.7	8.3	11.3	217.9
	OWL	7.9	10.0	48.1	8.5	11.2	120.3
	NEURONAL	7.9	10.2	44.7	8.6	11.1	109.9
Wanda	Uniform	8.8	11.2	72.1	8.4	11.5	146.0
	DSnoT	8.5	11.0	66.4	8.3	11.4	131.3
	OWL	7.6	9.8	47.6	7.5	10.2	98.0
	NEURONAL	7.6	9.9	46.8	7.6	10.3	90.3

A.2.5 NEURONAL on SparseGPT

In Tables 14-16, we present the results of NEURONAL on SparseGPT on the WikiText2, C4, and PTB datasets, using the *block-only* setting⁶.

Table 14: Perplexity on WikiText2 using SparseGPT.

Sparsity	Top-Up	Model				
		Phi-2.7B	LLama1 7B	LLama2 7B	Mistral-7B	OPT-6.7B
60%	Uniform	15.8	10.4	10.2	9.4	13.4
	OWL	15.8	9.4	9.2	9.1	14.2
	NEURONAL	15.7	9.9	9.3	9.1	13.7
70%	Uniform	28.9	27.3	27.3	22.0	20.5
	OWL	27.7	19.2	20.5	18.6	21.6
	NEURONAL	27.3	22.6	20.9	17.8	21.8
80%	Uniform	131.0	207.0	122.1	98.4	95.7
	OWL	107.5	93.8	84.3	77.2	80.8
	NEURONAL	113.5	144.7	88.7	70.8	84.0

Using SparseGPT, the superiority of NEURONAL is less evident than with other pruning algorithms. Nevertheless, NEURONAL turns out to be the best-performing top-up algorithm in 5 out of 15, 8 out of 15, and 7 out of 15 cases, respectively for WikiText2, C4, and PTB. Interestingly, for lower sparsity, the gap between uniform and non-uniform distribution (both NEURONAL and OWL) is less remarkable than at higher sparsity. We explain these results with the inherent functioning of SparseGPT, which, differently from the other pruning algorithms, includes a weight reconstruction step. However, we can conclude that also in this case, our proposed approach turns out to be effective in many cases at increasing the task performance.

⁶Since SparseGPT prunes and updates the weights from columns to rows, the row-wise step of NEURONAL cannot be included: indeed, it would force each row to have a different sparsity ratio, which is in contrast with the nature of SparseGPT.

Table 15: Perplexity on C4 using SparseGPT.

Sparsity	Top-Up	Model				
		Phi-2.7B	LLama1 7B	LLama2 7B	Mistral-7B	OPT-6.7B
60%	Uniform	19.0	12.8	12.9	13.0	15.3
	OWL	19.2	11.7	11.6	12.4	15.8
	NEURONAL	19.1	12.4	11.7	12.3	15.5
70%	Uniform	28.6	28.3	31.5	27.8	22.4
	OWL	28.2	21.1	22.8	23.7	22.4
	NEURONAL	27.8	23.8	22.5	21.9	22.2
80%	Uniform	98.7	136.2	104.8	86.5	72.5
	OWL	79.7	68.3	73.4	66.2	65.4
	NEURONAL	86.4	104.2	72.4	61.8	65.0

Table 16: Perplexity on PTB using SparseGPT.

Sparsity	Top-Up	Model				
		Phi-2.7B	LLama1 7B	LLama2 7B	Mistral-7B	OPT-6.7B
60%	Uniform	28.7	19.5	430.5	73.7	20.3
	OWL	29.3	16.9	262.1	70.9	21.0
	NEURONAL	28.2	18.2	249.2	67.2	20.6
70%	Uniform	50.3	52.6	3780.0	153.2	32.0
	OWL	51.0	37.0	1643.4	135.0	32.9
	NEURONAL	47.3	40.5	861.6	123.4	32.8
80%	Uniform	195.4	295.6	3201.7	316.2	102.3
	OWL	141.4	162.3	5556.5	278.8	98.9
	NEURONAL	156.7	260.2	3659.8	266.6	105.3

A.3 Block-only and Row-only Ablation

To complement the results presented in the main text on the C4 dataset, Tables 17-18 show the results of the ablation over the *block*-only and *row*-only steps also on WikiText2 and PTB. The results are in line with those obtained on C4.

Table 17: Ablation study: perplexity achieved when using the *block* and *row* steps alone over the WikiText2 dataset.

Sparsity	Top-Up	Model				
		Phi-2.7B	LLama1 7B	LLama2 7B	Mistral-7B	OPT-6.7B
60%	Uniform	25.8	10.7	10.8	11.3	15.2
	NEURONAL <i>block</i> -only	25.5	9.4	9.2	9.9	15.2
	NEURONAL <i>row</i> -only	25.8	11.2	11.4	11.3	16.5
	NEURONAL	25.2	9.6	9.4	9.9	16.3
70%	Uniform	227.6	85.1	78.0	60.7	157.5
	NEURONAL <i>block</i> -only	108.2	20.3	21.9	29.3	199.1
	NEURONAL <i>row</i> -only	200.4	85.3	75.5	60.7	116.8
	NEURONAL	89.9	21.5	23.9	29.0	183.9
80%	Uniform	20498.5	5219.5	4929.7	330.9	4259.6
	NEURONAL <i>block</i> -only	5637.9	458.9	439.9	205.9	1193.0
	NEURONAL <i>row</i> -only	11382.1	6715.8	916.8	330.9	4259.6
	NEURONAL	3873.6	376.1	213.9	226.3	988.2

Table 18: Ablation study: perplexity achieved when using the *block* and *row* steps alone over the PTB dataset.

Sparsity	Top-Up	Model				
		Phi-2.7B	LLama1 7B	LLama2 7B	Mistral-7B	OPT-6.7B
60%	Uniform	48.9	24.0	122.2	101.6	23.7
	NEURONAL <i>block</i> -only	41.9	16.7	65.6	74.6	23.5
	NEURONAL <i>row</i> -only	49.3	22.2	114.5	101.6	26.6
	NEURONAL	42.1	17.4	65.1	74.6	25.2
70%	Uniform	346.2	157.0	599.3	298.3	209.2
	NEURONAL <i>block</i> -only	152.5	41.4	209.7	196.9	250.0
	NEURONAL <i>row</i> -only	345.6	148.0	611.8	298.3	170.8
	NEURONAL	133.9	43.8	205.3	197.8	194.7
80%	Uniform	31362.6	10013.6	5285.2	783.7	2732.1
	NEURONAL <i>block</i> -only	6253.3	684.1	1295.2	723.0	1335.6
	NEURONAL <i>row</i> -only	18270.0	10008.4	2019.1	783.7	2732.1
	NEURONAL	6675.9	566.3	993.2	698.2	988.7

A.4 NEURONAL λ Selection

In the main text, we presented an experiment regarding the ability of NEURONAL to pick the most performing λ parameters (in the *block-only* cases) at 70% sparsity. Here we include the same analysis at 60% and 80% sparsity. In Fig.s 9-10, it is clearly visible how NEURONAL still performs correctly over different sparsity ratios. It is also worth noticing that the calibration data always come from the C4 dataset and then the results are transferred to the other unknown datasets.

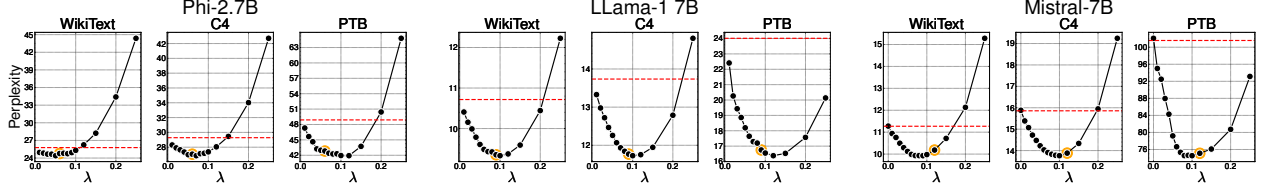


Figure 9: Perplexity over different values of λ at 60 % sparsity. The orange dot indicates the value selected by NEURONAL. The red line corresponds to the perplexity using a uniform distribution, hence $\lambda = 0$.

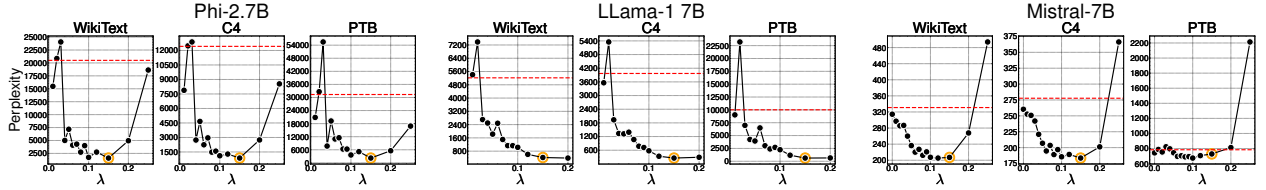


Figure 10: Perplexity over different values of λ at 80 % sparsity. The orange dot indicates the value selected by NEURONAL. The red line corresponds to the perplexity using a uniform distribution, hence $\lambda = 0$.

A.5 Calibration Data Ablation

In Tables 19-20, we complement the results regarding the seed set of the calibration data at 60% and 80% sparsity. The results are fully in line with the ones presented in the main text. As expected, the standard deviation of the performance increases when increasing the sparsity ratio and at higher sparsity (80%) it turns out to be model dependent.

We also conduct further experiments about the size of the calibration data ($|C_\lambda|$), see Fig. 11. Specifically, We compute the perplexity on WikiText2, C4, and PTB using different calibration data of different sizes (1, 2, 4, 8, 16 samples) in order to assess if the performance could be related to it. As clearly visible for almost all models, the performance is basically constant across the different calibration sizes. This does not apply only to OPT models, where for $|C_\lambda| = 16$ we reach the best performance by a large margin compared to $|C_\lambda| = 8$ (which is the standard value of $|C_\lambda|$ used in all the experiments), especially on WikiText2 and PTB. This, as pointed out in the main text, can better explain the reason why NEURONAL is able to outperform all the top-up competitors in Language Modeling but OPT.

Table 19: Ablation study: perplexity achieved by NEURONAL with different calibration data seeds (0, 16, 46) at 60% sparsity.

Dataset	Model				
	Phi-2.7B	LLama1 7B	LLama2 7B	Mistral-7B	OPT-6.7B
WikiText2	24.5 ± 0.6	9.5 ± 0.1	9.3 ± 0.0	10.1 ± 0.1	16.2 ± 0.1
C4	27.0 ± 0.2	11.9 ± 0.1	11.9 ± 0.0	13.8 ± 0.1	19.1 ± 0.1
PTB	42.3 ± 0.7	17.1 ± 0.3	65.3 ± 0.8	74.9 ± 0.2	25.1 ± 0.1

Table 20: Ablation study: perplexity achieved by NEURONAL with different calibration data seeds (0, 16, 46) at 80% sparsity.

Dataset	Model				
	Phi-2.7B	LLama1 7B	LLama2 7B	Mistral-7B	OPT-6.7B
WikiText2	3654.7 ± 255.1	382.4 ± 64.7	247.7 ± 29.4	216.5 ± 12.6	1284.9 ± 482.5
C4	72323.6 ± 121.7	250.5 ± 27.1	265.3 ± 34.1	171.7 ± 9.9	663.5 ± 316.3
PTB	6014.9 ± 788.3	624.4 ± 165.5	1101.9 ± 94.1	706.1 ± 6.9	1056.9 ± 124.5

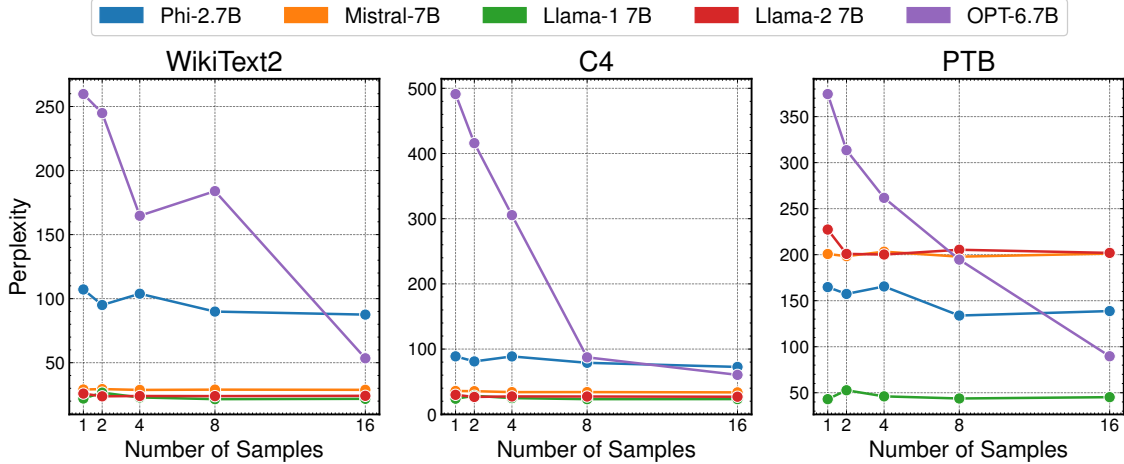


Figure 11: Perplexity over different values of $|C_\lambda|$ (size of the calibration data) when using NEURONAL on the 3 Language Modeling datasets at 70% sparsity.

A.6 NEURONAL λ Parameters

Here we show the λ parameters selected by our proposed approach for each model, sparsity ratio, and pruning algorithm tested in this work, aiming to facilitate the reproducibility of our results for the community. Please note that such values are the ones used for each combination sparsity-pruning algorithm-model that have been extracted from C_λ from C4 (using 0 as seed and 8 as size), and then transferred to all the other datasets/tasks. We report the final λ values for both the *block* and *row* steps in Table 21 for the first 5 models tested in the main text, and in Table 22 for the LLama-13B models.

Table 21: λ parameters selected by NEURONAL at sparsity xxx (block | row) for each combination sparsity-pruning algorithm-model. Note that for SparseGPT the *row* step is not possible (see the main text for details).

Sparsity	Top-Up	Model				
		Phi-2.7B	LLama1 7B	LLama2 7B	Mistral-7B	OPT-6.7B
60%	Magnitude	0.01 0.25	0.10 0.20	0.20 0.04	0.15 0.20	0.25 0.25
	Wanda	0.10 0.25	0.09 0.25	0.12 0.20	0.09 0.00	0.01 0.15
	MULTIFLOW	0.08 0.25	0.12 0.20	0.12 0.20	0.08 0.00	0.01 0.08
	SparseGPT	0.01 0.02	0.06 0.02	0.06 0.09	0.02 0.02	
70%	Magnitude	0.06 0.25	0.20 0.20	0.25 0.00	0.20 0.25	0.15 0.20
	Wanda	0.12 0.25	0.15 0.20	0.15 0.25	0.15 0.25	0.25 0.20
	MULTIFLOW	0.15 0.25	0.15 0.25	0.12 0.25	0.15 0.00	0.25 0.20
	SparseGPT	0.02 0.04	0.08 0.04	0.08 0.08	0.05 0.05	
80%	Magnitude	0.01 0.20	0.03 0.10	0.01 0.25	0.15 0.20	0.20 0.08
	Wanda	0.20 0.20	0.15 0.20	0.15 0.25	0.15 0.25	0.20 0.09
	MULTIFLOW	0.12 0.25	0.15 0.15	0.15 0.25	0.15 0.20	0.20 0.05
	SparseGPT	0.06 0.02	0.07 0.02	0.08 0.07	0.07 0.07	

Table 22: λ parameters selected by NEURONAL on the each combination sparsity-pruning algorithm for Llama-13B (V1 and V2) at sparsity xxx (block | row).

Sparsity	Top-Up	Model	
		LLama1 13B	LLama2 13B
60%	Magnitude	0.10 0.25	0.12 0.12
	Wanda	0.10 0.20	0.09 0.25
	MULTIFLOW	0.15 0.20	0.12 0.20
70%	Magnitude	0.12 0.25	0.25 0.25
	Wanda	0.15 0.25	0.12 0.20
	MULTIFLOW	0.15 0.15	0.15 0.25
80%	Magnitude	0.25 0.05	0.25 0.12
	Wanda	0.25 0.12	0.15 0.25
	MULTIFLOW	0.25 0.10	0.04 0.25